

# Geometric origin of superfluidity in the Lieb lattice flat band

Aleksi Julku,<sup>1</sup> Sebastiano Peotta,<sup>1</sup> Tuomas Vanhala,<sup>1</sup> Dong-Hee Kim,<sup>2</sup> and Päivi Törmä<sup>1,\*</sup>

<sup>1</sup>*COMP Centre of Excellence, Department of Applied Physics,  
Aalto University School of Science, FI-00076 Aalto, Finland*

<sup>2</sup>*Department of Physics and Photon Science, School of Physics and Chemistry,  
Gwangju Institute of Science and Technology, Gwangju 61005, Korea*

The ground state and transport properties of the Lieb lattice flat band in the presence of an attractive Hubbard interaction are considered. It is shown that the superfluid weight can be large even for an isolated and strictly flat band. Moreover the superfluid weight is proportional to the interaction strength and to the quantum metric, a band structure invariant obtained from the flat-band Bloch functions. These predictions are amenable to verification with ultracold gases and may explain the anomalous behaviour of the superfluid weight of high- $T_c$  superconductors.

A flat band is a Bloch band where the energy dispersion  $\varepsilon_{n\mathbf{k}} \approx \varepsilon_n$  ( $n$  is the band index) is constant as a function of quasi-momentum  $\mathbf{k}$  and is composed of localized eigenstates. In absence of disorder and interactions the ground state of a flat band is insulating at any filling [1]. However, interactions and disorder lead to a ground state reconstruction and it is often hard to predict its properties. Bands that are nearly flat and/or feature nontrivial topological invariant, similar to Landau levels producing the quantum Hall effects [2–4], are the subject of current research both theoretically [5–12] and can be experimentally studied with ultracold gases [13–15]. A vast literature on flat-band ferromagnetism has developed starting with the works of Lieb [16] and, subsequently, Tasaki and Mielke [17–20]. More recently, the high density of states of flat bands has been predicted to provide a dramatic enhancement of the superconducting critical temperature [21, 22]. Indeed, for fixed interaction strength, the flat-band dispersion provides the maximal critical temperature within mean-field BCS theory [23].

Flat bands, or quasi-flat bands, can be realized in bipartite lattices [16] and other models [6–8, 20, 24]. One of the simplest bipartite lattice featuring a strictly flat band is the Lieb lattice [Fig. 1(a)]. Most of the recent studies on models defined on the Lieb lattice focus on the ferromagnetic and topological properties [27–32], while superconductivity in the Lieb lattice has been studied in Refs. [30, 33]. On the experimental side, a highly tunable Lieb lattice has been realized with ultracold gases [34]. Intriguingly, the  $\text{CuO}_2$  planes responsible for the exotic properties of high- $T_c$  cuprate superconductors have the structure of the Lieb lattice. Thus a Hubbard model on the Lieb lattice [35–38] is a natural, and possibly indispensable, extension of the single-band Hubbard model that is commonly used to describe these systems [39].

The important question of whether an isolated strictly flat band can support superfluid transport is open. Its answer is of interest for ongoing ultracold gas experiments and may have important implications for the theory of superconductivity. Meissner effect and dissipationless transport are manifestations of a finite superfluid weight that in conventional superconductors at zero

temperature reads  $D_s = n_p/m_{\text{eff}}$ , with  $n_p$  the particle density and  $m_{\text{eff}}$  the effective mass of the approximately parabolic band. Interestingly, the superfluid weight of a flat band is not necessarily vanishing, as suggested by the diverging effective mass  $m_{\text{eff}} \rightarrow +\infty$ , but proportional to another band structure invariant, the quantum metric integrated over the Brillouin zone [40]. Flat bands with nonzero Chern number  $C$  (the same topological index as characterizes Landau levels) are guaranteed to have nonzero superfluid weight according to the lower bound  $D_s \geq |C|$ . For a large class of Hamiltonians defined on the Lieb lattice the flat band has  $C = 0$  [41]. Lower bounds on  $D_s$  are not available at present for topologically trivial bands or bands characterized by other topological invariants than the Chern number.

Here we consider a tight-binding model with attractive Hubbard interaction defined on the Lieb lattice. This model features a strictly flat band with zero Chern number. We show that the total superfluid weight tensor receives contributions from the flat band,  $D_s|_{\text{f.b.}}$ , and from the other bands,  $D_s|_{\text{o.b.}}$ , that is,  $D_s = D_s|_{\text{f.b.}} + D_s|_{\text{o.b.}}$ . We find that  $D_s|_{\text{f.b.}}$  depends on the flat-band Bloch functions through the quantum metric. This is called a “geometric” contribution distinct from the “conventional” contribution, which depends only on the derivatives of the band dispersion [40]. To our knowledge only the latter one is accounted for when evaluating the superfluid weight of known superconductors [42, 43]. Importantly, the energy scale of the geometric contribution is the coupling constant  $U$ , at odds with the conventional result  $D_s = n_p/m_{\text{eff}} \propto J$ , where  $J$  is the characteristic hopping energy scale in a tight-binding Hamiltonian. We identify the regimes where  $D_s|_{\text{f.b.}}$  dominates over the term  $D_s|_{\text{o.b.}}$ , which includes the conventional and geometric contributions of other bands. These results are obtained with mean-field BCS theory. This is appropriate here since we show that the BCS wavefunction is an exact ground state in a large class of interacting Hamiltonians with flat bands. The validity of BCS theory is further confirmed by dynamical mean-field theory (DMFT) and exact diagonalization (ED).

*Hubbard model on the Lieb lattice* — The Hamiltonian

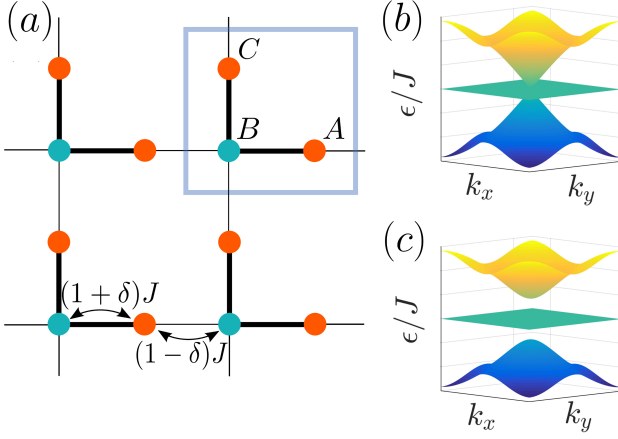


FIG. 1. (a) Lieb lattice with its three-site unit cell shown (grey box). The orbitals in the unit cell are labelled by  $\alpha = A, B, C$ . The thick lines represent nearest-neighbour hoppings with energy  $(1+\delta)J$ , while the hopping energy corresponding to the thin lines is  $(1-\delta)J$  with  $0 \leq \delta \leq 1$  parametrizing the staggered hopping. (b)-(c) The energy dispersion as a function of quasimomentum  $\mathbf{k}$  for  $\delta = 0$  (b) and  $\delta = 0.3$  (c), respectively. The middle band is strictly flat  $\epsilon_{0\mathbf{k}} = 0$  for any value of  $\delta$  while the upper and lower band have dispersions  $\epsilon_{\pm, \mathbf{k}} = \pm 2J\sqrt{1+\delta^2 + (1-\delta^2)(\cos k_x a + \cos k_y a)}/2$ .

$\hat{H} = \hat{H}_{\text{kin}} + \hat{H}_{\text{int}} - \mu\hat{N}$  defined on the Lieb lattice comprises the chemical potential term  $-\mu\hat{N}$  ( $\hat{N}$  is the particle number operator), the attractive Hubbard interaction  $\hat{H}_{\text{int}}$  defined below and the kinetic term  $\hat{H}_{\text{kin}} = \sum_{\mathbf{k}, \sigma} \hat{c}_{\mathbf{k}\sigma}^\dagger H_{\mathbf{k}} \hat{c}_{\mathbf{k}\sigma}$  with staggered nearest-neighbour hopping [see Fig. 1 (a)]

$$H_{\mathbf{k}} = 2J \begin{pmatrix} 0 & a_{\mathbf{k}} & 0 \\ a_{\mathbf{k}}^* & 0 & b_{\mathbf{k}} \\ 0 & b_{\mathbf{k}}^* & 0 \end{pmatrix}, \quad (1)$$

where  $a_{\mathbf{k}} = \cos \frac{k_x a}{2} + i\delta \sin \frac{k_x a}{2}$ ,  $b_{\mathbf{k}} = \cos \frac{k_y a}{2} + i\delta \sin \frac{k_y a}{2}$  and  $a$  the lattice constant. The fermion operators are defined as  $\hat{\mathbf{c}}_{\mathbf{k}\sigma} = (\hat{c}_{A\mathbf{k}\sigma}, \hat{c}_{B\mathbf{k}\sigma}, \hat{c}_{C\mathbf{k}\sigma})^T$  and  $\hat{c}_{\alpha\mathbf{k}\sigma} = \frac{1}{\sqrt{N_c}} \sum_{\mathbf{i}} e^{i\mathbf{k}\cdot\mathbf{r}_{\mathbf{i}\alpha}} \hat{c}_{\mathbf{i}\alpha\sigma}$  where  $N_c$  is the number of unit cells,  $\mathbf{r}_{\mathbf{i}\alpha}$  is the position vector of the  $\alpha$  orbital in the  $\mathbf{i}$ -th unit cell [ $\mathbf{i} = (i_x, i_y)^T$ ] and the operator  $\hat{c}_{\mathbf{i}\alpha\sigma}$  annihilates a fermion with spin  $\sigma = \uparrow, \downarrow$  in the orbital centered at  $\mathbf{r}_{\mathbf{i}\alpha}$ . By diagonalizing  $H_{\mathbf{k}} = \mathcal{G}_{\mathbf{k}} \epsilon_{\mathbf{k}} \mathcal{G}_{\mathbf{k}}^\dagger$  we obtain the dispersions of the middle  $\epsilon_{0\mathbf{k}} = 0$  and upper and lower bands  $\epsilon_{\pm, \mathbf{k}} = -\epsilon_{-, \mathbf{k}}$ , collected in a diagonal matrix  $\epsilon_{\mathbf{k}} = \text{diag}(\epsilon_{n\mathbf{k}})$ , and a unitary matrix  $\mathcal{G}_{\mathbf{k}}$  whose columns are the Bloch functions  $g_{n\mathbf{k}}(\alpha) = [\mathcal{G}_{\mathbf{k}}]_{\alpha, n}$ . The middle band  $n = 0$  is strictly flat for any value of the staggered-hopping parameter  $\delta$  and isolated from the other bands by an energy gap  $E_{\text{gap}} = \sqrt{8}J\delta$ . The parameter  $\delta$  regularizes the singularities occurring due to the band intersection for  $\delta = 0$ . As in Ref. [33], the interaction term  $\hat{H}_{\text{int}} = -U \sum_{\mathbf{i}, \alpha} (\hat{n}_{\mathbf{i}\alpha\uparrow} - 1/2)(\hat{n}_{\mathbf{i}\alpha\downarrow} - 1/2)$ , where  $U > 0$  and  $\hat{n}_{\mathbf{i}\alpha\sigma} = \hat{c}_{\mathbf{i}\alpha\sigma}^\dagger \hat{c}_{\mathbf{i}\alpha\sigma}$ , is approximated by mean-field pairing

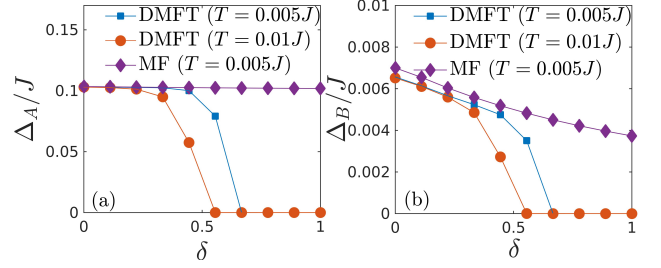


FIG. 2. Order parameters  $\Delta_A/J$  (left) and  $\Delta_B/J$  (right) as a function of  $\delta$  obtained with DMFT and mean-field at temperatures  $k_B T = 5 \cdot 10^{-3}J$  and  $10^{-2}J$ , filling  $\nu = 1.5$  and coupling strength  $U = 0.4J$ . At these temperatures, significantly lower than the mean-field critical temperature  $k_B T_{c, \text{MF}} \approx \Delta_A/2 = U n_\phi/4 = 5 \cdot 10^{-2}J$ , the mean-field results are indistinguishable from the zero temperatures ones.

$$\Delta_\alpha = -U \langle \hat{c}_{\mathbf{i}\alpha\downarrow} \hat{c}_{\mathbf{i}\alpha\uparrow} \rangle \text{ and Hartree potentials } n_\alpha = \langle \hat{n}_{\mathbf{i}\alpha\sigma} \rangle$$

$$\hat{H}_{\text{int}} \approx \sum_{\mathbf{i}, \alpha} \left( \Delta_\alpha \hat{c}_{\mathbf{i}\alpha\uparrow}^\dagger \hat{c}_{\mathbf{i}\alpha\downarrow}^\dagger + \text{H.c.} \right) + U \sum_{\mathbf{i}, \alpha, \sigma} \left( n_\alpha - \frac{1}{2} \right) \hat{n}_{\mathbf{i}\alpha\sigma}. \quad (2)$$

The equivalence of orbitals  $A$  and  $C$  implies  $\Delta_A = \Delta_C$  and  $n_A = n_C$ . The self-consistent equations for  $\Delta_\alpha$  and  $n_\alpha$  have a simple form at half-filling  $\nu = \sum_\alpha n_\alpha = 1.5$  [44]. At leading order in  $U/J$  and zero temperature one has  $\Delta_A = U n_\phi/2 + O(U^2/J)$  and  $\Delta_B = O(U^2/J)$  with  $n_\phi^{-1} = 2$  the number of orbitals on which the flat band states are nonvanishing ( $A$  and  $C$  orbitals).

*Exactness of BCS wavefunction for a flat band* — We provide here an argument showing that the BCS wavefunction is an exact ground state in an isolated flat band ( $U \ll E_{\text{gap}}$ ) in the case of an attractive Hubbard interaction. This result generalizes the one for the special case of the Harper-Hubbard model given in Ref. [40], for details see Ref. [44]. In a *repulsive* Hubbard model with a partially-filled flat band the ferromagnetic wavefunction  $|\text{Ferro}\rangle = \prod_{\mathbf{k}} (u c_{\bar{n}\mathbf{k}\downarrow}^\dagger + v c_{\bar{n}\mathbf{k}\uparrow}^\dagger) |0\rangle$  is an exact ground state [19, 20] (here  $|u|^2 + |v|^2 = 1$  and  $c_{\bar{n}\mathbf{k}\sigma}^\dagger$  creates a fermion within the flat band) because of no competition between kinetic and interaction energies. Due to the flat band dispersion it is possible to perform a particle-hole transformation  $\hat{c}_{\bar{n}\mathbf{k}\downarrow} \rightarrow \hat{c}_{\bar{n}(-\mathbf{k})\downarrow}^\dagger$  to map  $|\text{Ferro}\rangle$  into a BCS wavefunction  $|\text{BCS}\rangle = \prod_{\mathbf{k}} (u + v c_{\bar{n}\mathbf{k}\uparrow}^\dagger c_{\bar{n}(-\mathbf{k})\downarrow}^\dagger) |0\rangle$  [45, 46], now an exact ground state for a flat band with an *attractive* Hubbard interaction. The finite superfluid weight (see below) guarantees stability of the BCS ground state. *Comparison with DMFT* — To investigate the accuracy of the BCS theory also for a nonisolated flat band, we compare in Fig. 2 mean-field theory with DMFT with respect to the pairing potentials (order parameters)  $\Delta_A$  [Fig. 2 (a)] and  $\Delta_B$  [Fig. 2 (b)] as a function of  $\delta$  at half filling. Specifically, we use cellular dynamical mean-field theory with continuous-time interaction-expansion impurity solver [47]. Our DMFT calculation treats quantum

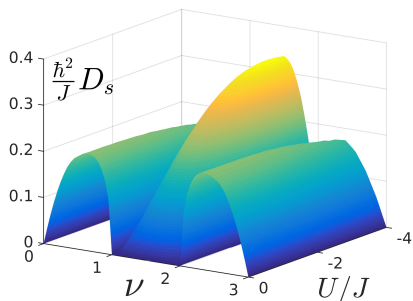


FIG. 3. Diagonal components of the superfluid weight tensor  $[D_s]_{x,x} = [D_s]_{y,y} \sim D_s$  as a function of interaction  $U/J$  and filling  $\nu$  for  $\delta = 10^{-3}$  and at zero temperature. The superfluid weight for partially filled flat band ( $1 \leq \nu \leq 2$ ) depends strongly on the interaction strength  $U$ , whereas for the other bands it is essentially constant.

correlations exactly within the three-site unit cell and thereby goes beyond BCS mean-field theory. For small  $\delta$ , DMFT is in good agreement with mean-field theory, especially regarding  $\Delta_A$ . The results for large  $\delta$  will be discussed below. In particular, both methods show that, even when  $\delta = E_{\text{gap}} = 0$ , pairing is strongly dominated by the flat band and the effect of the other bands is small.

*Superfluid weight* — The superfluid weight is defined as the change in free energy density  $\Delta f = \frac{1}{8} D_s (\hbar \mathbf{q})^2$  due to the winding with wavevector  $\mathbf{q}$  of the order parameter phase  $\Delta(\mathbf{r}) = \Delta e^{2i\mathbf{q}\cdot\mathbf{r}}$ . We calculate it using multiband BCS theory and show in Fig. 3 as a function of coupling  $U$  and filling  $\nu$  for zero temperature and  $\delta = 10^{-3}$  [44]. For  $\delta \neq 0$ , the superfluid weight tensor acquires nonzero off-diagonal components  $[D_s]_{x,y} = [D_s]_{y,x}$ . However, this effect is small and we focus only on the diagonal components  $[D_s]_{x,x} = [D_s]_{y,y} \sim D_s$ . A striking feature is that, for partially filled dispersive bands,  $D_s$  is finite and roughly constant as a function of  $U$ , while the superfluid weight of the partially filled flat band depends strongly on  $U$  and has a nonmonotonic behavior [see also Fig. 4(a)]. This is consistent with the fact that superconductivity in the dispersive bands emerges from a metallic state with nonzero Drude weight which is the  $U \rightarrow 0$  limit of  $D_s$  at zero temperature [48, 49]. On the contrary, superconductivity in the flat band smoothly emerges with increasing  $U$  from an *insulating* state with zero Drude weight. Notably, the superfluid weight of a topologically trivial flat band can be nonzero and larger than the one of dispersive bands in the same model.

This peculiar behaviour is a consequence of the geometric origin of superfluidity in the flat band. The total superfluid weight can be split in conventional and geometrical contribution  $D_s = D_{s,\text{conv}} + D_{s,\text{geom}}$ . The conventional contribution  $D_{s,\text{conv}}$  depends only on the derivatives of the dispersions  $\varepsilon_{n\mathbf{k}}$  while the geometric one  $D_{s,\text{geom}}$  includes derivatives of the Bloch functions  $g_{n\mathbf{k}}$  and scales with  $\Delta_A = \Delta_C$  in this specific model [44].

Obviously the flat band does not contribute to the conventional term, while  $D_{s,\text{geom}} = D_{s,\text{geom}}|_{\text{f.b.}} + D_{s,\text{geom}}|_{\text{o.b.}}$  can be further split into a term originating purely from the flat band  $D_{s,\text{geom}}|_{\text{f.b.}} = D_s|_{\text{f.b.}}$  and the remaining part  $D_{s,\text{geom}}|_{\text{o.b.}}$ , which includes the geometric effect of the other bands. All three terms  $D_{s,\text{conv}}$ ,  $D_{s,\text{geom}}|_{\text{f.b.}}$  and  $D_{s,\text{geom}}|_{\text{o.b.}}$  are invariant with respect to the gauge freedom consisting in the multiplication of the Bloch functions by an arbitrary  $\mathbf{k}$ -dependent phase factor and are thus well-defined. In our model the flat-band term  $D_s|_{\text{f.b.}}$  has the form

$$[D_s]_{i,j}|_{\text{f.b.}} = \frac{1}{\pi \hbar^2} \frac{\Delta_A^2}{E_0} \tanh \frac{\beta E_0}{2} \mathcal{M}_{ij}^R|_{\text{f.b.}}. \quad (3)$$

Here  $E_0 = \sqrt{\mu^2 + \Delta_A^2}$ ,  $\beta = 1/(k_B T)$  is the inverse temperature and  $\mathcal{M}_{ij}^R|_{\text{f.b.}} = (2\pi)^{-1} \int_{\text{B.Z.}} d^2\mathbf{k} \text{Re } \mathcal{B}_{ij}(\mathbf{k})|_{\text{f.b.}}$ . The matrix  $\mathcal{M}_{ij}^R|_{\text{f.b.}}$  is the Brillouin-zone integral of the real part of the quantum geometric tensor  $\mathcal{B}_{ij}(\mathbf{k})$ , also called quantum metric [1, 25, 26],

$$\mathcal{B}_{ij}(\mathbf{k})|_{\text{f.b.}} = 2 \langle \partial_{k_i} g_{0\mathbf{k}} | (1 - |g_{0\mathbf{k}}\rangle \langle g_{0\mathbf{k}}|) | \partial_{k_j} g_{0\mathbf{k}} \rangle, \quad (4)$$

with  $g_{0\mathbf{k}}(\alpha) = \langle \alpha | g_{0\mathbf{k}} \rangle$  the flat-band Bloch functions. At half-filling one has  $\mu = 0$  and  $\Delta_A = \frac{U n_\phi}{2} \tanh \frac{\beta \Delta_A}{2} + O(U^2/J)$ , and Eq. (3) can be further simplified.

The strong dependence of  $D_s$  on  $U$  for a partially filled flat band originates from the geometric term as shown in Figs. 4(a)-(b) where  $D_{s,\text{conv}}$  and  $D_{s,\text{geom}}$  are presented as a function of  $U$  for half-filled flat band [ $\nu = 1.5$ , Fig. 4(a)] and half-filled upper band [ $\nu = 2.5$ , Fig. 4(b)]. For  $\nu = 1.5$  the term  $D_{s,\text{geom}}$  dominates  $D_{s,\text{conv}}$ , while for  $\nu = 2.5$   $D_{s,\text{geom}}$  is negligible in the weak coupling regime.

In addition, we perform ED calculations for Drude weight  $D$  [51] on the 12-site cluster displayed in Fig. 1(a) with periodic boundary conditions. In the bulk limit, it is known that  $D$  is equivalent to  $D_s$  for a gapped system [48–50]. While our system size is small, which possibly affects the difference from the mean-field  $D_s$  in the noninteracting limit shown in Fig. 4(a), their overall qualitative agreement is notable. In Fig. 4(a) both are peaked at  $U \sim 4J$  and then decrease with increasing  $U$ .

In Figs. 4(c)-(d) we compare the conventional term  $D_{s,\text{conv}}$ , the flat-band contribution  $D_s|_{\text{f.b.}}$  and the geometric contribution due to the other bands  $D_{s,\text{geom}}|_{\text{o.b.}}$  at half-filling  $\nu = 1.5$  and for small  $U \leq 0.2J$ . Two values of  $\delta$  are shown:  $\delta = 5 \cdot 10^{-3}$  [Fig. 4(c)] and  $\delta = 0.1$  [Fig. 4(d)]. In both cases  $D_{s,\text{conv}}$  is negligible due to the vanishing density of states of the dispersive bands, while  $D_s|_{\text{f.b.}}$  gives the dominant contribution, linear in  $U$ . The geometric contribution of the other bands,  $D_{s,\text{geom}}|_{\text{o.b.}}$ , is negative and less relevant when the flat band becomes more isolated for larger  $\delta$ . When  $U$  increases, the negative contribution of  $D_{s,\text{geom}}|_{\text{o.b.}}$  becomes more prominent and for very large  $U$  it cancels the positive contribution of  $D_{s,\text{geom}}|_{\text{f.b.}}$  [see Fig. 4(a)]. This means that pairing has to occur in a *subset* of all bands for  $D_{s,\text{geom}}$  to manifest,

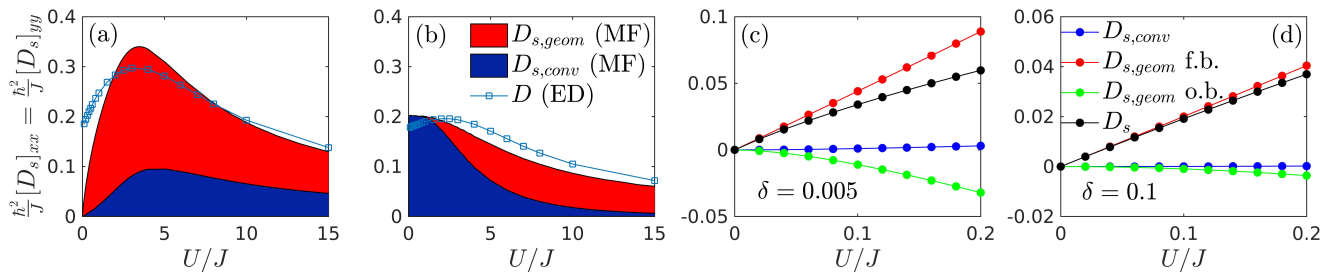


FIG. 4. (a)-(b) Conventional superfluid weight  $D_{s,\text{conv}}$  (blue area) compared with the geometric one  $D_{s,\text{geom}}$  (red area) for  $\nu = 1.5$  (a) and  $\nu = 2.5$  (b). Here  $T = 0$  and  $\delta = 10^{-3}$ . Also the Drude weight  $D_s$  obtained from exact diagonalization is depicted (squares). (c)-(d) Various superfluid weight contributions for half-filled flat band, small  $U \leq 0.2J$ ,  $\delta = 5 \cdot 10^{-3}$  (c),  $\delta = 0.1$  (d).

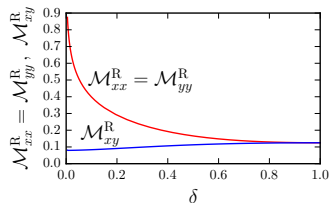


FIG. 5. Brillouin-zone integral of the flat-band quantum metric  $\mathcal{M}_{ij}^R$  as a function of  $\delta$ . The diagonal components have a logarithmic singularity at  $\delta = 0$ .

and it explains the decreasing trend of  $D_s$  in Figs. 4(a)-4(b). As shown in Fig. 5, the invariant  $\mathcal{M}_{ij}^R|_{\text{f.b.}}$  diverges at  $\delta = 0$ , thus the slope of  $D_s$  as a function of  $U$  is infinite at  $U = 0$ . However for any finite value of  $U$  we have verified that this divergence is cured by  $D_{s,\text{geom}}|_{\text{o.b.}}$ . Thus for  $\delta = 0$  superfluidity has a truly multiband character. In the opposite limit  $\delta \rightarrow 1$  one eigenvalue of  $\mathcal{M}_{ij}^R|_{\text{f.b.}}$  becomes zero and superfluidity is lost, consistently with the fact that the unit cells become decoupled [see Fig. 1(a)]. The DMFT results in Fig. 2 seem to capture this behavior, in contrast to mean-field theory which gives a finite order parameter even for  $\delta = 1$ .

*Discussion* — The main result of this work is that topologically trivial flat bands are promising for hosting a high-temperature superconductor, in the same way as topologically nontrivial ones. Indeed a flat band dispersion allows to optimize not only the MF critical temperature [23], but also the superfluid weight [see Figs. 4(a)-(b)]. The superfluid weight affects the critical temperature in two dimensions through the Berezinsky-Kosterlitz-Thouless (BKT) transition. We show that the superfluid weight has geometric origin, i.e. it is proportional to the quantum metric of the flat band [Eqs. (3)-(4)]. The fingerprint of the geometric origin is the strong dependence of  $D_s$  on the coupling constant  $U$ , which could be observed in ultracold gases where the interaction is easily tunable.

Achieving the superfluid phase of an ultracold gas in an optical lattice is difficult, due to the still too high

temperatures (specific entropies) that can be attained with current methods [52, 53]. We find the BKT transition temperature in the Lieb lattice to be  $k_B T_{c,\text{BKT}} = 0.133J$  [44] at the optimal coupling  $U \approx 4J$  [Fig. 4(a)]. It can be compared with the optimal Néel temperature for the 3D repulsive Fermi-Hubbard model  $k_B T_{\text{Néel}} = 0.333(7)J$  [54], which is at the verge of experimental capabilities [53]. The critical temperatures are substantially higher in three dimensions where, in contrast to the BKT estimate in 2D, one can use the mean-field one. We find the mean-field estimate  $k_B T_{c,\text{MF}} \approx 0.5 - 0.8J$  (for  $U \approx 4J$ ,  $\nu = 1.5$ ). In general, flat bands optimize the critical temperature, indeed we find  $T_{c,\text{BKT}}$  for the flat band superfluid twice as high compared to the dispersive bands in our model.

Finally, it is an intriguing question whether the geometric contribution to the superfluid weight plays a role in known high- $T_c$  superconductors. Several reasons suggest such connection: i) the geometric term  $D_{s,\text{geom}} \propto \Delta \propto T_c$  is expected to be more important with increasing  $T_c$ ; ii) the  $T = 0$  superfluid weight in cuprates scales with  $T_c$  (Uemura relation [55, 56]), a feature that can be explained by the presence of the geometric contribution, independently of the specific pairing mechanism; iii) the  $\text{CuO}_2$  planes in cuprates form a Lieb lattice and there are indications that a three-orbital Hubbard model may be needed for capturing, even qualitatively, the superconducting properties [38, 57, 58]. Note that the geometric superfluid weight term is absent in the standard single-orbital Hubbard model, since the Bloch functions are trivial, but necessarily present in the three-orbital model and this may be a deciding feature in favor of the latter. Further work is needed along this research line.

This work was supported by the Academy of Finland through its Centres of Excellence Programme (2012-2017) and under Project Nos. 263347, 251748, and 272490, and by the European Research Council (ERC-2013-AdG-340748-CODE). We acknowledge useful discussions with Jildou Baarsma, Jami Kinnunen and Long Liang. S. P. thanks Shunji Tsuchiya for sharing his unpublished data, and both him and Wilhelm Zwirger



for interesting discussions. T.I.V. is grateful for the support from the Vilho, Yrjö and Kalle Väisälä Foundation. D.H.K. acknowledges support from the National Research Foundation of Korea through its Basic Science Research Program (NRF-2014R1A1A1002682, NRF-2015K2A7A1035792). Computing resources were provided by CSC – the Finnish IT Centre for Science and the Triton cluster at Aalto University.

---

\* [paivi.torma@aalto.fi](mailto:paivi.torma@aalto.fi)

- [1] R. Resta, The insulating state of matter: a geometrical theory, *Eur. Phys. J. B* **79**, 121137 (2011).
- [2] *The Quantum Hall Effect*, R. E. Prange, S. M. Girvin, eds., 2nd edition, Springer-Verlag New York (1990).
- [3] *The Quantum Hall Effects*, T. Chakraborty, P. Pietiläinen, 2nd edition, Springer-Verlag Berlin-Heidelberg (1995).
- [4] *Perspectives in Quantum Hall Effects: Novel Quantum Liquids in Low Dimensional Semiconductor Structures*, S. das Sarma, A. Pinczuk, eds., Wiley-VCH Verlag (2004).
- [5] S. D. Huber, E. Altman, Bose condensation in flat bands, *Phys. Rev. B* **82**, 184502 (2010).
- [6] K. Sun, Z. Gu, H. Katsura, S. Das Sarma, Nearly flat-bands with nontrivial topology, *Phys. Rev. Lett.* **106**, 236803 (2011).
- [7] E. Tang, J.-W. Mei, X.-G. Wen, High-temperature fractional quantum Hall states, *Phys. Rev. Lett.* **106**, 236802 (2011).
- [8] T. Neupert, L. Santos, C. Chamon, C. Mudry, Fractional quantum Hall states at zero magnetic field *Phys. Rev. Lett.* **106**, 236804 (2011).
- [9] E. J. Breholtz, Z. Liu, Topological flat band models and fractional Chern insulators, *Int. J. Mod. Phys. B* **27**, 1330017 (2013).
- [10] R. Roy, Band geometry of fractional topological insulators, *Phys. Rev. B* **90**, 165139 (2014).
- [11] S. Takayoshi, H. Katsura, N. Watanabe, H. Aoki, Phase diagram and pair Tomonaga-Luttinger liquid in a Bose-Hubbard model with flat bands, *Phys. Rev. A* **88**, 063613 (2013).
- [12] M. Tovmasyan, E. P. L. van Nieuwenburg, S. D. Huber, Geometry-induced pair condensation, *Phys. Rev. B* **88**, 220510 (2013).
- [13] M. Aidelsburger, M. Atala, M. Lohse, J. T. Barreiro, B. Paredes, I. Bloch, Realization of the Hofstadter Hamiltonian with ultracold atoms in optical lattices, *Phys. Rev. Lett.* **111**, 185301 (2013).
- [14] H. Miyake, G. A. Siviloglou, C. J. Kennedy, W. C. Burton, W. Ketterle, Realizing the Harper Hamiltonian with laser-assisted tunneling in optical lattices, *Phys. Rev. Lett.* **111**, 185302 (2013).
- [15] M. Aidelsburger, et al., Measuring the Chern number of Hofstadter bands with ultracold bosonic atoms, *Nature Physics* **11**, 162166 (2015).
- [16] E. H. Lieb, Two theorems on the Hubbard model, *Phys. Rev. Lett.* **62**, 1201 (1989).
- [17] A. Mielke, Ferromagnetic ground states for the Hubbard model on line graphs, *J. Phys. A: Math. Gen.* **24**, L73 (1991); Ferromagnetism in the Hubbard model on line graphs and further considerations, *J. Phys. A: Math. Gen.* **24**, 3311 (1991).
- [18] H. Tasaki, Ferromagnetism in the Hubbard models with degenerate single-electron ground states, *Phys. Rev. Lett.* **69**, 1608 (1992).
- [19] A. Mielke, H. Tasaki, Ferromagnetism in the Hubbard model, *Comm. Math. Phys.* **158**, 341 (1993).
- [20] H. Tasaki, From Nagaoka’s ferromagnetism to flat-band ferromagnetism and beyond, *Prog. Theor. Phys.* **99** (4), 489-548 (1998).
- [21] N. B. Kopnin, T. T. Heikkilä, G. E. Volovik, High-temperature surface superconductivity in topological flat-band systems, *Phys. Rev. B* **83**, 220503(R) (2011).
- [22] T. T. Heikkilä, N. B. Kopnin, G. E. Volovik, Flat bands in topological media, *JETP Letters* **94**, Issue 3, 233-239 (2011).
- [23] K. Noda, K. Inaba, M. Yamashita, BCS superconducting transitions in lattice fermions, [arXiv:1512.07858](https://arxiv.org/abs/1512.07858).
- [24] C. Weeks, M. Franz, Topological insulators on the Lieb and perovskite lattices, *Phys. Rev. B* **82**, 085310 (2010).
- [25] J. P. Provost, G. Vallee, Riemannian structure on manifolds of quantum states, *Commun. Math. Phys.* **76**, 289 (1980).
- [26] M. V. Berry, “The quantum phase, five years after”, pp. 7-28 in *Geometric phases in physics*, eds. A. Shapere & F. Wilczek, World Scientific (1989).
- [27] K. Noda, A. Koga, N. Kawakami, T. Pruschke, Ferromagnetism of cold fermions loaded into a decorated square lattice, *Phys. Rev. A* **80**, 063622 (2009).
- [28] N. Goldman, D. F. Urban, D. Bercioux, Topological phases for fermionic cold atoms on the Lieb lattice, *Phys. Rev. A* **83**, 063601 (2011).
- [29] K. Noda, K. Inaba, M. Yamashita, Flat-band ferromagnetism in the multilayer Lieb optical lattice, *Phys. Rev. A* **90**, 043624 (2014).
- [30] K. Noda, K. Inaba, M. Yamashita, Magnetism in the three-dimensional layered Lieb lattice: Enhanced transition temperature via flat-band and Van Hove singularities, *Phys. Rev. A* **91**, 063610 (2015).
- [31] W.-F. Tsai, C. Fang, H. Yao, J. Hu, Interaction-driven topological and nematic phases on the Lieb lattice, *New J. Phys.* **17** 055016 (2015).
- [32] G. Palumbo, K. Meichanetzidis, Two-dimensional Chern semimetals on the Lieb lattice, *Phys. Rev. B* **92**, 235106 (2015).
- [33] V. I. Iglovikov, F. Hébert, B. Grémaud, G. G. Batrouni, R. T. Scalettar, Superconducting transitions in flat-band systems, *Phys. Rev. B* **90**, 094506 (2014).
- [34] S. Taie, H. Ozawa, T. Ichinose, T. Nishio, S. Nakajima, Y. Takahashi, Coherent driving and freezing of bosonic matter wave in an optical Lieb lattice, *Science Advances*, Vol. **1**, no. 10, e1500854 (2015).
- [35] L. F. Mattheiss, Electronic band properties and superconductivity in  $\text{La}_{2-y}\text{X}_y\text{CuO}_4$ , *Phys. Rev. Lett.* **58**, 1028 (1987).
- [36] C. M. Varma, S. Schmitt-Rink, E. Abrahams, Charge transfer excitations and superconductivity in “ionic” metals, *Solid State Commun.* **62**, 681 (1987).
- [37] V. J. Emery, Theory of high- $T_c$  superconductivity in oxides, *Phys. Rev. Lett.* **58**, 2794 (1987).
- [38] Y. F. Kung, et al., Characterizing the three-orbital Hubbard model with determinant quantum Monte Carlo, [arXiv:1601.05421](https://arxiv.org/abs/1601.05421).

- [39] J. P. F. LeBlanc, et al., Solutions of the two-dimensional Hubbard model: benchmarks and results from a wide range of numerical algorithms, *Phys. Rev. X* **5**, 041041 (2015).
- [40] S. Peotta, P. Törmä, Superfluidity in topologically non-trivial flat bands, *Nature Communications* **6**, 8944 (2015).
- [41] L. Chen, T. Mazaheri, A. Seidel, X. Tang, The impossibility of exactly flat non-trivial Chern bands in strictly local periodic tight binding models, *J. Phys. A: Math. Theor.* **47** 152001 (2014).
- [42] R. Prozorov, R. Giannetta, Magnetic penetration depth in unconventional superconductors, *Supercond. Sci. Technol.* **19**, R41R67 (2006).
- [43] R. Prozorov, V. G. Kogan, London penetration depth in iron-based superconductors, *Rep. Prog. Phys.* **74**, 124505 (2011).
- [44] See Supplemental Material at [link](#) where we provide more details and analytical results on the mean-field theory used for obtaining the superfluid weight. Furthermore we discuss in detail the argument showing that the BCS wavefunction is an exact ground state in a flat band and provide additional DMFT data and the estimate of the BKT critical temperature.
- [45] S. M. Girvin, A. H. MacDonald, “Multicomponent Quantum Hall Systems: The Sum of Their Parts and More”, p. 161 in *Perspectives in Quantum Hall Effects*, eds. S. Das Sarma & A. Pinczuk, Wiley-VCH (2004).
- [46] Y. N. Joglekar, A. H. MacDonald, Microscopic functional integral theory of quantum fluctuations in double-layer quantum Hall ferromagnets, *Phys. Rev. B* **64**, 155315 (2001).
- [47] T. I. Vanhala, J. E. Baarsma, M. O. J. Heikkinen, M. Troyer, A. Harju, P. Törmä, Superfluidity and density order in a bilayer extended Hubbard model, *Phys. Rev. B* **91**, 144510 (2015)
- [48] D. J. Scalapino, S. R. White, S.-C. Zhang, Superfluid density and the Drude weight of the Hubbard model, *Phys. Rev. Lett.* **68**, 2830 (1992).
- [49] D. J. Scalapino, S. R. White, S.-C. Zhang, Insulator, metal, or superconductor: the criteria, *Phys. Rev. B* **47**, 7995 (1993).
- [50] P. J. H. Denteneer, Superfluid density in the two-dimensional attractive Hubbard model: quantitative estimates, *Phys. Rev. B* **49**, 6364 (1994).
- [51] E. Dagotto, A. Moreo, F. Ortolani, J. Riera, D. J. Scalapino, Optical conductivity of the two-dimensional Hubbard model, *Phys. Rev. B* **45**, 10107 (1992).
- [52] T. Esslinger, Fermi-Hubbard Physics with Atoms in an Optical Lattice, *Ann. Rev. Cond. Mat. Phys.* **1**, 129-152 (2010).
- [53] R. Jördens et al., Quantitative determination of temperature in the approach to magnetic order of ultracold fermions in an optical lattice, *Phys. Rev. Lett.* **104**, 180401 (2010).
- [54] S. Fuchs, E. Gull, L. Pollet, E. Burovski, E. Kozik, T. Pruschke, M. Troyer, Thermodynamics of the 3D Hubbard model on approaching the Néel transition, *Phys. Rev. Lett.* **106**, 030401 Published 18 January 2011.
- [55] Y. J. Uemura et al., Universal correlations between  $T_c$  and  $n_s/m^*$  (carrier density over effective mass) in high- $T_c$  cuprate superconductors, *Phys. Rev. Lett.* **62**, 2317 (1989).
- [56] P. A. Marchetti, G. Bighin, Gauge approach to superfluid density in underdoped cuprates, *Europ. Phys. Lett.*, **110** 37001 (2015), and references therein.
- [57] V. V. Val'kov, D. M. Dzebisashvili, M. M. Korovushkin, A. F. Barabanov, Stability of the superconducting  $d_{x^2-y^2}$ -wave pairing towards the intersite Coulomb repulsion between oxygen holes in high- $T_c$  superconductors, [arXiv:1601.06894](#).
- [58] C. P. J. Adolphs, S. Moser, G. A. Sawatzky, M. Berciu, Non-Zhang-Rice singlet character of the first ionization state of T-CuO, [arXiv:1602.01113](#).

## Appendix A: Multiband BCS approach and superfluid weight

### 1. Bogoliubov de-Gennes Hamiltonian

In order to calculate the superfluid weight we use the multiband BCS theory developed in Ref. [1], which is a mean field (MF) approach, with the difference that we take into account the Hartree potentials  $n_\alpha = \langle \hat{n}_{i\alpha\sigma} \rangle$  ( $\alpha \in \{A, B, C\}$ ) of Eq. (2) in the main text, as explained below. Furthermore, the Lieb lattice geometry, related orbitals and band structures are used. The general procedure is repeated here for completeness. The starting point is the MF Bogoliubov-de Gennes Hamiltonian  $\bar{H}_{\mathbf{k}}(\mathbf{q})$  in the presence of a pairing amplitude  $\Delta(\mathbf{r}) = \Delta e^{2i\mathbf{q}\cdot\mathbf{r}}$  with finite phase winding given by the wavevector  $\mathbf{q}$ . This nonuniform phase describes a state with a finite supercurrent. The corresponding Bogoliubov-de Gennes Hamiltonian is

$$\bar{H}_{\mathbf{k}}(\mathbf{q}) = \begin{pmatrix} \varepsilon_{\mathbf{k}-\mathbf{q}} - \mu\mathbf{1} & \mathcal{G}_{\mathbf{k}-\mathbf{q}}^\dagger \Delta \mathcal{G}_{\mathbf{k}+\mathbf{q}} \\ \mathcal{G}_{\mathbf{k}+\mathbf{q}}^\dagger \Delta \mathcal{G}_{\mathbf{k}-\mathbf{q}} & -(\varepsilon_{\mathbf{k}+\mathbf{q}} - \mu\mathbf{1}) \end{pmatrix}, \quad \text{with} \quad \Delta = \begin{pmatrix} \Delta_A & 0 & 0 \\ 0 & \Delta_B & 0 \\ 0 & 0 & \Delta_A \end{pmatrix}. \quad (5)$$

Note that the Bogoliubov-de Gennes Hamiltonian is a  $2 \times 2$  block matrix, where the diagonal matrices of the band dispersions  $\varepsilon_{\mathbf{k}} = \text{diag}(\varepsilon_{n\mathbf{k}})$  and the unitary matrix of the Bloch functions  $g_{n\mathbf{k}}(\alpha) = [\mathcal{G}_{\mathbf{k}}]_{\alpha,n}$  are obtained by diagonalizing the kinetic single-particle Hamiltonian  $H_{\mathbf{k}} = \mathcal{G}_{\mathbf{k}} \varepsilon_{\mathbf{k}} \mathcal{G}_{\mathbf{k}}^\dagger$ . The notation  $[M]_{a,b}$  for the matrix elements of a matrix  $M$  is used throughout. The kinetic single-particle Hamiltonian reads

$$H_{\mathbf{k}} = 2J \begin{pmatrix} \gamma_A/2 & a_{\mathbf{k}} & 0 \\ a_{\mathbf{k}}^* & \gamma_B/2 & b_{\mathbf{k}} \\ 0 & b_{\mathbf{k}}^* & \gamma_A/2 \end{pmatrix}. \quad (6)$$

This is the same as Eq. (1) in the main text with the only difference that the Hartree potential  $\gamma_\alpha = -U/J(n_\alpha - 1/2)$  has been included. Then the energy dispersions and the Bloch functions in the presence of a finite Hartree term are

$$\varepsilon_{\mathbf{k}} = \begin{pmatrix} \varepsilon_{+, \mathbf{k}} & & \\ & J\gamma_A & \\ & & \varepsilon_{-, \mathbf{k}} \end{pmatrix} \quad (7)$$

$$\varepsilon_{\pm, \mathbf{k}} = J(\gamma_A + \gamma_B) \pm 2J\sqrt{(\gamma_A + \gamma_B)^2 + |a_{\mathbf{k}}|^2 + |b_{\mathbf{k}}|^2} \quad (8)$$

$$\mathcal{G}_{\mathbf{k}} = \begin{pmatrix} \frac{a_{\mathbf{k}}}{\sqrt{2\chi_{\mathbf{k}} + 2(\gamma_A - \gamma_B)\sqrt{\chi_{\mathbf{k}}}}} & -\frac{b_{\mathbf{k}}}{\sqrt{|a_{\mathbf{k}}|^2 + |b_{\mathbf{k}}|^2}} & \frac{a_{\mathbf{k}}}{\sqrt{2\chi_{\mathbf{k}} - 2(\gamma_A - \gamma_B)\sqrt{\chi_{\mathbf{k}}}}} \\ \frac{-\gamma_A + \gamma_B - \sqrt{\chi_{\mathbf{k}}}}{\sqrt{2\chi_{\mathbf{k}} + 2(\gamma_A - \gamma_B)\sqrt{\chi_{\mathbf{k}}}}} & 0 & \frac{-\gamma_A + \gamma_B + \sqrt{\chi_{\mathbf{k}}}}{\sqrt{2\chi_{\mathbf{k}} - 2(\gamma_A - \gamma_B)\sqrt{\chi_{\mathbf{k}}}}} \\ \frac{b_{\mathbf{k}}^*}{\sqrt{2\chi_{\mathbf{k}} + 2(\gamma_A - \gamma_B)\sqrt{\chi_{\mathbf{k}}}}} & \frac{a_{\mathbf{k}}^*}{\sqrt{|a_{\mathbf{k}}|^2 + |b_{\mathbf{k}}|^2}} & \frac{b_{\mathbf{k}}^*}{\sqrt{2\chi_{\mathbf{k}} - 2(\gamma_A - \gamma_B)\sqrt{\chi_{\mathbf{k}}}}} \end{pmatrix}, \quad (9)$$

where  $\chi_{\mathbf{k}} = (\gamma_A - \gamma_B)^2 + |a_{\mathbf{k}}|^2 + |b_{\mathbf{k}}|^2$ . Note that the Hartree potential has the effect of shifting the flat band energy, but the flat-band Bloch functions (the middle column of Eq. (9)) are unaffected.

In general the pairing potentials  $\Delta_\alpha$  and the Hartree potentials  $n_\alpha$  have to be found self-consistently for any value of  $\mathbf{q}$ . According to Ref. [1] it is necessary to find the self-consistent solution only for  $\mathbf{q} = 0$  in order to calculate the superfluid density. The diagonalization of Eq. (5) for  $\mathbf{q} = 0$  provides the quasiparticle energies ( $E_{n\mathbf{k}}$ ) and wavefunctions ( $\mathcal{W}_{\mathbf{k}}$ )

$$\bar{H}_{\mathbf{k}}(\mathbf{q} = 0) = \mathcal{W}_{\mathbf{k}}(\mathbf{q} = 0) E_{\mathbf{k}}(\mathbf{q} = 0) \mathcal{W}_{\mathbf{k}}^\dagger(\mathbf{q} = 0), \quad (10)$$

with

$$E_{\mathbf{k}}(\mathbf{q} = 0) = \begin{pmatrix} E_{\mathbf{k}}^> & 0 \\ 0 & -E_{\mathbf{k}}^> \end{pmatrix} = \begin{pmatrix} \text{diag}(E_{n\mathbf{k}}) & 0 \\ 0 & -\text{diag}(E_{n\mathbf{k}}) \end{pmatrix} \quad (11)$$

and

$$\mathcal{W}_{\mathbf{k}}(\mathbf{q} = 0) = \begin{pmatrix} \mathcal{U}_{\mathbf{k}} & -\mathcal{V}_{\mathbf{k}} \\ \mathcal{V}_{\mathbf{k}} & \mathcal{U}_{\mathbf{k}} \end{pmatrix}. \quad (12)$$

We use the notation  $\mathcal{U}_{\mathbf{k}}$ ,  $\mathcal{V}_{\mathbf{k}}$  for the blocks of  $\mathcal{W}_{\mathbf{k}}(\mathbf{q} = 0)$  as a reminder that these are the generalization for a multiband Bogoliubov-de Gennes Hamiltonian of the usual BCS coherence factors  $u_{\mathbf{k}}$ ,  $v_{\mathbf{k}}$  [2]. In Eq. (11) the diagonal matrix  $E_{\mathbf{k}}^>$  contains the positive quasiparticle energies  $E_{n\mathbf{k}} \geq 0$ .

## 2. General expression for the superfluid weight tensor in a multiband system

For convenience we define the following quantities:

$$\mathcal{D}_{\mathbf{k}}(\mathbf{q}) = -\mathcal{G}_{\mathbf{k}-\mathbf{q}}^\dagger \Delta \mathcal{G}_{\mathbf{k}+\mathbf{q}} = \mathcal{D}_{\mathbf{k}}^\dagger(-\mathbf{q}) \quad (13)$$

$$N_{\mathbf{k},i} = \mathcal{W}_{\mathbf{k}}^\dagger(\mathbf{q}=0) \partial_{q_i} \bar{H}_{\mathbf{k}}(\mathbf{q}=0) \mathcal{W}_{\mathbf{k}}(\mathbf{q}=0) = \begin{pmatrix} A_{\mathbf{k},i} & B_{\mathbf{k},i} \\ -B_{\mathbf{k},i} & A_{\mathbf{k},i} \end{pmatrix} \quad (14)$$

$$\text{with } \begin{cases} A_{\mathbf{k},i} = \mathcal{U}_{\mathbf{k}}^\dagger \partial_{k_i} \varepsilon_{\mathbf{k}} \mathcal{U}_{\mathbf{k}} + \mathcal{V}_{\mathbf{k}}^\dagger \partial_{k_i} \varepsilon_{\mathbf{k}} \mathcal{V}_{\mathbf{k}} + \mathcal{U}_{\mathbf{k}}^\dagger \partial_{q_i} \mathcal{D}_{\mathbf{k}}(\mathbf{q}=0) \mathcal{V}_{\mathbf{k}} - \mathcal{V}_{\mathbf{k}}^\dagger \partial_{q_i} \mathcal{D}_{\mathbf{k}}(\mathbf{q}=0) \mathcal{U}_{\mathbf{k}} \\ B_{\mathbf{k},i} = \mathcal{U}_{\mathbf{k}}^\dagger \partial_{q_i} \mathcal{D}_{\mathbf{k}}(\mathbf{q}=0) \mathcal{U}_{\mathbf{k}} + \mathcal{V}_{\mathbf{k}}^\dagger \partial_{q_i} \mathcal{D}_{\mathbf{k}}(\mathbf{q}=0) \mathcal{V}_{\mathbf{k}} + \mathcal{V}_{\mathbf{k}}^\dagger \partial_{k_i} \varepsilon_{\mathbf{k}} \mathcal{U}_{\mathbf{k}} - \mathcal{U}_{\mathbf{k}}^\dagger \partial_{k_i} \varepsilon_{\mathbf{k}} \mathcal{V}_{\mathbf{k}} \end{cases} \quad (14)$$

$$[T_{\mathbf{k}}]_{a,b} = \begin{cases} \left[ \frac{\beta}{2 \cosh^2(\beta E_{\mathbf{k}}/2)} \right]_{a,a} & \text{for } a = b, \\ \frac{[\tanh(\beta E_{\mathbf{k}}/2)]_{a,a} - [\tanh(\beta E_{\mathbf{k}}/2)]_{b,b}}{[E_{\mathbf{k}}]_{a,a} - [E_{\mathbf{k}}]_{b,b}} & \text{for } a \neq b. \end{cases} \quad (15)$$

Using these definitions it is possible to derive the following result for the superfluid weight tensor  $[D_s]_{i,j}$

$$[D_s]_{i,j} = \frac{1}{V \hbar^2} \left. \frac{\partial^2 \Omega}{\partial q_i \partial q_j} \right|_{\mu, \Delta, \mathbf{q}=0} = [D_{s,\text{conv}}]_{i,j} + [D_{s,\text{geom}}]_{i,j}, \quad \text{with} \quad (16)$$

$$[D_{s,\text{conv}}]_{i,j} = \frac{2}{V \hbar^2} \sum_{\mathbf{k}} \text{Tr} \left[ \left( \mathcal{V}_{\mathbf{k}} \frac{1}{e^{-\beta E_{\mathbf{k}}} + 1} \mathcal{V}_{\mathbf{k}}^\dagger + \mathcal{U}_{\mathbf{k}} \frac{1}{e^{\beta E_{\mathbf{k}}} + 1} \mathcal{U}_{\mathbf{k}}^\dagger \right) \partial_{k_i} \partial_{k_j} \varepsilon_{\mathbf{k}} \right], \quad (17)$$

$$[D_{s,\text{geom}}]_{i,j} = \frac{1}{V \hbar^2} \left\{ 2 \sum_{\mathbf{k}} \text{Tr} \left[ \left( \mathcal{U}_{\mathbf{k}} \mathcal{V}_{\mathbf{k}}^\dagger - \mathcal{U}_{\mathbf{k}} \frac{1}{e^{\beta E_{\mathbf{k}}} + 1} \mathcal{V}_{\mathbf{k}}^\dagger - \mathcal{V}_{\mathbf{k}} \frac{1}{e^{-\beta E_{\mathbf{k}}} + 1} \mathcal{U}_{\mathbf{k}}^\dagger \right) \partial_{q_i} \partial_{q_j} \mathcal{D}_{\mathbf{k}}(\mathbf{q}=0) \right] \right. \\ \left. - \frac{1}{2} \sum_{\mathbf{k}} \sum_{a,b} [T_{\mathbf{k}}]_{a,b} [N_{\mathbf{k},i}]_{a,b} [N_{\mathbf{k},j}]_{b,a} \right\}. \quad (18)$$

The superfluid weight tensor is defined as the derivatives with respect to  $\mathbf{q}$  of the grand potential  $\Omega(\mu, T, \Delta, \mathbf{q})$  and  $V$  is the system volume (area in 2D). We use here a different notation than in Ref. [1]: the conventional contribution to the superfluid weight  $D_{s,\text{conv}}$  is called  $D_{s,1}$  in Ref. [1], while the geometric one  $D_{s,\text{geom}}$  corresponds to  $D_{s,2} + D_{s,3}$  in the same reference. The conventional contribution is distinguished by the fact that only the derivatives of the band dispersion enter in Eq. (17), while in the geometric one also the derivatives of the Bloch functions appear through the quantities  $\partial_{q_i} \mathcal{D}_{\mathbf{k}}(\mathbf{q}=0)$ ,  $\partial_{q_i} \partial_{q_j} \mathcal{D}_{\mathbf{k}}(\mathbf{q}=0)$ , where  $\mathcal{D}_{\mathbf{k}}(\mathbf{q})$  is defined in Eq. (13). Moreover, the only energy scale of the conventional contribution is the hopping energy  $J$ , which is the scale of the band dispersion  $\varepsilon_{\mathbf{k}}$ . On the other hand,  $D_{s,\text{geom}}$  depends also on the energy gaps  $\Delta_\alpha$  again through  $\mathcal{D}_{\mathbf{k}}(\mathbf{q})$ .

## 3. Changing the filling within the flat band

As the formulas for the superfluid weight are derived in the grand canonical ensemble, the chemical potential  $\mu$  is fixed rather than the total filling  $\nu = \sum_\alpha n_\alpha$ . In case of dispersive bands we can scan the filling by simply changing the chemical potential. However, in case of the flat band the same chemical potential  $\mu = 0$  corresponds to an arbitrary partial filling of the flat band, namely the filling  $\nu(\mu)$  as a function of  $\mu$  is discontinuous at  $\mu = 0$ . In order to obtain the superfluid weight as a function of filling presented in Fig. 3 of the main text, we exploit the fact that once a self-consistent solution for  $\mu = 0$  is found, which corresponds to a partially filled flat band, it is possible to obtain another self-consistent solution by an arbitrary rotation of the following three dimensional vectors [3]

$$\mathbf{S}_\alpha = \left( \text{Re} \left[ \frac{\Delta_\alpha}{-U} \right], \text{Im} \left[ \frac{\Delta_\alpha}{-U} \right], n_\alpha - \frac{1}{2} \right). \quad (19)$$

The rotation is the same for all sublattices labelled by  $\alpha$ . This is a fundamental symmetry of any bipartite lattice and it can be better appreciated by performing the particle-hole transformation introduced by Emery that maps the attractive Hubbard model into the repulsive one [4]. In the case of the repulsive Hubbard model, this symmetry corresponds to rotations of the magnetization vector. Note that this symmetry holds only if the pairing potentials  $\Delta_\alpha$  and Hartree potentials  $n_\alpha$  are treated on an equal footing. This is one reason to introduce the Hartree potential. By employing this symmetry, we are able to obtain the superfluid weight for any filling of the flat band.



#### 4. Analytical results for half-filled flat band

In general we adopt a fully numerical approach to solve the self-consistent equations given in Ref. [1] and evaluating Eqs. (16)-(18) to obtain the superfluid weight. However, it turns out that an analytical solution can be found when the flat band is half-filled. The theorem of Ref. [5] guarantees that the Hartree potential vanishes precisely at half-filling ( $n_\alpha - 1/2 = 0 = \gamma_\alpha$ ). The quasiparticle energies, the eigenvalues of (5), take a very simple form at half filling

$$E_{\pm, \mathbf{k}} = \sqrt{\epsilon_{\mathbf{k}}^2 + \Delta_s^2} \pm |\Delta_d| \geq 0, \quad E_{0, \mathbf{k}} = \Delta_A, \quad E_{\mathbf{k}}^> = \text{diag}(E_{+, \mathbf{k}}, E_{0, \mathbf{k}}, E_{-, \mathbf{k}}), \quad (20)$$

where  $\Delta_d = (\Delta_A - \Delta_B)/2$ ,  $\Delta_s = (\Delta_A + \Delta_B)/2$  and  $\epsilon_{\mathbf{k}} = 2J\sqrt{|a_{\mathbf{k}}|^2 + |b_{\mathbf{k}}|^2}$ . Correspondingly, the unitary matrix  $\mathcal{W}_{\mathbf{k}}$  that diagonalizes the BdG Hamiltonian reads

$$\mathcal{W}_{\mathbf{k}} = \begin{pmatrix} \mathcal{U}_{\mathbf{k}} & -\mathcal{V}_{\mathbf{k}} \\ \mathcal{V}_{\mathbf{k}} & \mathcal{U}_{\mathbf{k}} \end{pmatrix}, \quad \mathcal{U}_{\mathbf{k}} = \frac{1}{\sqrt{2}} \begin{pmatrix} \cos \frac{\phi_{\mathbf{k}}}{2} & 0 & -\cos \frac{\phi_{\mathbf{k}}}{2} \\ 0 & 1 & 0 \\ \sin \frac{\phi_{\mathbf{k}}}{2} & 0 & \sin \frac{\phi_{\mathbf{k}}}{2} \end{pmatrix}, \quad \mathcal{V}_{\mathbf{k}} = \frac{1}{\sqrt{2}} \begin{pmatrix} \sin \frac{\phi_{\mathbf{k}}}{2} & 0 & -\sin \frac{\phi_{\mathbf{k}}}{2} \\ 0 & 1 & 0 \\ \cos \frac{\phi_{\mathbf{k}}}{2} & 0 & \cos \frac{\phi_{\mathbf{k}}}{2} \end{pmatrix}. \quad (21)$$

Here the coefficients of  $\mathcal{U}_{\mathbf{k}}$  and  $\mathcal{V}_{\mathbf{k}}$  take precisely the form of BCS coherence factors

$$\cos \frac{\phi_{\mathbf{k}}}{2} = \frac{1}{\sqrt{2}} \sqrt{1 + \frac{\epsilon_{\mathbf{k}}}{\sqrt{\epsilon_{\mathbf{k}}^2 + \Delta_s^2}}}, \quad \sin \frac{\phi_{\mathbf{k}}}{2} = \frac{1}{\sqrt{2}} \sqrt{1 - \frac{\epsilon_{\mathbf{k}}}{\sqrt{\epsilon_{\mathbf{k}}^2 + \Delta_s^2}}}. \quad (22)$$

Away from half-filling the block structure of  $\mathcal{U}_{\mathbf{k}}$  and  $\mathcal{V}_{\mathbf{k}}$  survives, namely the flat band, which corresponds to the middle  $1 \times 1$  block in Eq. (21), is decoupled from the other bands for any filling and the corresponding  $2 \times 2$  Bogoliubov-de Gennes Hamiltonian can be trivially solved. This is a peculiar feature of our model, which implies that there is a flat band of quasiparticle excitations. We use this decomposition to provide the result in Eq. (3) in the main text (see below). However, away from half-filling it is not easy to provide a simple solution for the remaining  $4 \times 4$  block in the Bogoliubov-de Gennes Hamiltonian corresponding to the other bands.

Given the above results for the eigenvectors  $\mathcal{W}_{\mathbf{k}}$  and the eigenvalues  $E_{n\mathbf{k}}$ , the only ingredient needed for the evaluation of the superfluid weight are the derivatives of the matrix  $\mathcal{D}_{\mathbf{k}}(\mathbf{q}) = -\mathcal{G}_{\mathbf{k}-\mathbf{q}}^\dagger \Delta \mathcal{G}_{\mathbf{k}+\mathbf{q}}$ . Let us introduce a two-component complex spinor  $|s_{\mathbf{k}}\rangle$  and its partner obtained by the time-reversal symmetry  $|\bar{s}_{\mathbf{k}}\rangle$

$$|s_{\mathbf{k}}\rangle = \frac{1}{\sqrt{|a_{\mathbf{k}}|^2 + |b_{\mathbf{k}}|^2}} \begin{pmatrix} a_{\mathbf{k}} \\ b_{\mathbf{k}}^* \end{pmatrix}, \quad |\bar{s}_{\mathbf{k}}\rangle = \mathcal{T} |s_{\mathbf{k}}\rangle = i\sigma_y \mathcal{C} |s_{\mathbf{k}}\rangle = \frac{1}{\sqrt{|a_{\mathbf{k}}|^2 + |b_{\mathbf{k}}|^2}} \begin{pmatrix} b_{\mathbf{k}} \\ -a_{\mathbf{k}}^* \end{pmatrix}. \quad (23)$$

Here  $\mathcal{T} = i\sigma_y \mathcal{C}$  is the time reversal operator and  $\mathcal{C}$  is the complex conjugate operator. It follows from the definitions that  $\langle s_{\mathbf{k}} | \bar{s}_{\mathbf{k}} \rangle = 0$ . The spinor  $|s_{\mathbf{k}}\rangle$  is a purely formal construction and does not have any direct physical meaning. Using these definitions the matrix  $\mathcal{G}_{\mathbf{k}_1}^\dagger \Delta \mathcal{G}_{\mathbf{k}_2}$  can be represented as

$$\mathcal{G}_{\mathbf{k}_1}^\dagger \Delta \mathcal{G}_{\mathbf{k}_2} = \frac{\Delta_A}{2} \begin{pmatrix} \langle s_{\mathbf{k}_1} | s_{\mathbf{k}_2} \rangle & \sqrt{2} \langle s_{\mathbf{k}_1} | \bar{s}_{\mathbf{k}_2} \rangle & \langle s_{\mathbf{k}_1} | s_{\mathbf{k}_2} \rangle \\ \sqrt{2} \langle \bar{s}_{\mathbf{k}_1} | s_{\mathbf{k}_2} \rangle & 2 \langle \bar{s}_{\mathbf{k}_1} | \bar{s}_{\mathbf{k}_2} \rangle & \sqrt{2} \langle \bar{s}_{\mathbf{k}_1} | s_{\mathbf{k}_2} \rangle \\ \langle s_{\mathbf{k}_1} | s_{\mathbf{k}_2} \rangle & \sqrt{2} \langle s_{\mathbf{k}_1} | \bar{s}_{\mathbf{k}_2} \rangle & \langle s_{\mathbf{k}_1} | s_{\mathbf{k}_2} \rangle \end{pmatrix} + \frac{\Delta_B}{2} \begin{pmatrix} 1 & 0 & -1 \\ 0 & 0 & 0 \\ -1 & 0 & 1 \end{pmatrix}. \quad (24)$$

Note that the matrix  $\mathcal{G}_{\mathbf{k}_1}^\dagger \Delta \mathcal{G}_{\mathbf{k}_2}$  is the sum of two terms proportional to the order parameters  $\Delta_A$  and  $\Delta_B$ , respectively. Only the term proportional to  $\Delta_A$  depends on the wavevectors  $\mathbf{k}_{1,2}$ . Therefore the derivatives of the matrix  $\mathcal{D}_{\mathbf{k}}(\mathbf{q}) = -\mathcal{G}_{\mathbf{k}-\mathbf{q}}^\dagger \Delta \mathcal{G}_{\mathbf{k}+\mathbf{q}}$  are equal to the derivatives of  $\mathcal{D}'_{\mathbf{k}}(\mathbf{q}) = -\Delta_A \mathcal{G}_{\mathbf{k}-\mathbf{q}}^\dagger \mathcal{G}_{\mathbf{k}+\mathbf{q}}$ , i.e. one can set  $\Delta_B = \Delta_A$  for the purpose of calculating derivatives. As shown in Ref. [1], this provides a number of simplifications. This is a unique property of the Lieb lattice which does not hold in general. As a consequence only the energy scale  $\Delta_A = \Delta_C$  enters in the geometric contribution to the superfluid weight, but not  $\Delta_B$ . It is interesting to note that the flat band states are supported only on the  $A, C$  sublattices but not on the  $B$  sublattice [3]. Another advantage of Eq. (24) is that the calculation of the derivatives of the six independent matrix elements of a  $3 \times 3$  hermitian matrix is reduced to the calculation of the derivatives of only two quantities, namely  $\langle s_{\mathbf{k}_1} | s_{\mathbf{k}_2} \rangle = \langle \bar{s}_{\mathbf{k}_1} | \bar{s}_{\mathbf{k}_2} \rangle^*$  and  $\langle s_{\mathbf{k}_1} | \bar{s}_{\mathbf{k}_2} \rangle = -\langle \bar{s}_{\mathbf{k}_1} | s_{\mathbf{k}_2} \rangle^*$ . The quantum geometric tensor of the flat band reads in the spinor notation

$$\mathcal{B}_{ij}(\mathbf{k})|_{\text{f.b.}} = 2 \langle \partial_{k_i} \bar{s}_{\mathbf{k}} | s_{\mathbf{k}} \rangle \langle s_{\mathbf{k}} | \partial_{k_j} \bar{s}_{\mathbf{k}} \rangle = 2 \langle \partial_{k_j} s_{\mathbf{k}} | \bar{s}_{\mathbf{k}} \rangle \langle \bar{s}_{\mathbf{k}} | \partial_{k_i} s_{\mathbf{k}} \rangle = 2 \langle \partial_{k_i} g_{0\mathbf{k}} | (1 - |g_{0\mathbf{k}}\rangle \langle g_{0\mathbf{k}}|) | \partial_{k_j} g_{0\mathbf{k}} \rangle. \quad (25)$$

The real part of the quantum geometric tensor  $\mathcal{B}_{ij}(\mathbf{k})$  is called the quantum metric.

### 5. Gap equations at half filling

Using Eqs. (21)-(22) and the general results of Ref. [1] one obtains the gap equations

$$\Delta_A = \Delta_C = \frac{U}{4N_c} \sum_{\mathbf{k}} [t_{+,\mathbf{k}} \sin \phi_{\mathbf{k}} + t_{-,\mathbf{k}}] + \frac{U}{4} \tanh \frac{\beta \Delta_A}{2}, \quad (26)$$

$$\Delta_B = \frac{U}{2N_c} \sum_{\mathbf{k}} [t_{+,\mathbf{k}} \sin \phi_{\mathbf{k}} - t_{-,\mathbf{k}}], \quad (27)$$

$$\text{with } t_{\pm,\mathbf{k}} = \frac{1}{2} \left( \tanh \frac{\beta E_{+,\mathbf{k}}}{2} \pm \tanh \frac{\beta E_{-,\mathbf{k}}}{2} \right). \quad (28)$$

Here  $N_c$  is the number of unit cells in the lattice. In the zero temperature limit ( $t_{+,\mathbf{k}} \rightarrow 1$ ,  $\tanh(\beta \Delta_A/2) \rightarrow 1$ ,  $t_{-,\mathbf{k}} \rightarrow 0$ ) the gap equations read

$$\Delta_A = \Delta_C = \frac{U}{4N_c} \sum_{\mathbf{k}} \frac{\Delta_s}{\sqrt{\epsilon_{\mathbf{k}}^2 + \Delta_s^2}} + \frac{U}{4}, \quad (29)$$

$$\Delta_B = \frac{U}{2N_c} \sum_{\mathbf{k}} \frac{\Delta_s}{\sqrt{\epsilon_{\mathbf{k}}^2 + \Delta_s^2}}. \quad (30)$$

The gap equations for the two order parameters  $\Delta_A$  and  $\Delta_B$  are coupled since  $\Delta_s = (\Delta_A + \Delta_B)/2$ . The flat band provides  $\mathbf{k}$ -independent terms in the gap equations for the order parameter  $\Delta_A = \Delta_C$ , namely the term  $\frac{U}{4} \tanh \frac{\beta \Delta_A}{2}$  in Eq. (26) and  $\frac{U}{4}$  in Eq. (29) (highlighted in red). It makes sense that the flat band enters only in the equations for the order parameter  $\Delta_A$  but not  $\Delta_B$  since the flat band is composed of states that are completely localized in the  $A, C$  sublattices [3]. From the zero temperature gap equations the asymptotic behaviour of the order parameters for small  $U$  is derived

$$\Delta_A \approx \frac{n_\phi U}{2} \left( 1 + \frac{U}{8J} I(\delta) \right) \quad \text{with } n_\phi^{-1} = 2, \quad \Delta_B \approx \Delta_A \frac{U}{4J} I(\delta) \approx \frac{n_\phi U^2}{8J} I(\delta). \quad (31)$$

The constant  $I(\delta)$  is defined by

$$I(\delta) = \frac{J}{N_c} \sum_{\mathbf{k}} \frac{1}{\epsilon_{\mathbf{k}}} = \int_0^{2\pi} dx \int_0^{2\pi} dy \frac{1}{2\sqrt{1 + \delta^2 + \frac{1-\delta^2}{2}(\cos x + \cos y)}}. \quad (32)$$

For the value  $\delta = 10^{-3}$  used in most of the calculations one obtains  $I(\delta) \approx 0.64$ . The leading order result for  $\Delta_A = n_\phi U/2$  agrees with the general result in the isolated flat-band case [1], where  $n_\phi^{-1} = 2$  is the number of orbitals (sublattices) on which the flat-band states have nonvanishing amplitude.

### 6. Superfluid weight at half filling

Using Eqs. (21)-(22) and after a straightforward but tedious calculation, one can derive the following expression for the superfluid weight as a summation (integral) of a function of  $\mathbf{k}$  over the whole Brillouin zone ( $A = N_c a^2$  is the system area,  $a$  the lattice constant)

$$\begin{aligned} [D_s]_{i,j} = \frac{1}{A\hbar^2} \sum_{\mathbf{k}} \left[ -2t_{+,\mathbf{k}} \cos \phi_{\mathbf{k}} \partial_{k_i} \partial_{k_j} \epsilon_{\mathbf{k}} - \frac{4t_{-,\mathbf{k}}}{E_{+,\mathbf{k}} - E_{-,\mathbf{k}}} \partial_{k_i} \epsilon_{\mathbf{k}} \partial_{k_j} \epsilon_{\mathbf{k}} \right. \\ \left. + 2\Delta_A \left( \tanh \frac{\beta \Delta_A}{2} + t_{+,\mathbf{k}} \sin \phi_{\mathbf{k}} + t_{-,\mathbf{k}} \right) (\langle \partial_{k_i} s_{\mathbf{k}} | \partial_{k_j} s_{\mathbf{k}} \rangle + \langle \partial_{k_j} s_{\mathbf{k}} | \partial_{k_i} s_{\mathbf{k}} \rangle) \right. \\ \left. - \Delta_A^2 \langle \partial_{k_i} s_{\mathbf{k}} | s_{\mathbf{k}} \rangle \langle s_{\mathbf{k}} | \partial_{k_j} s_{\mathbf{k}} \rangle f(\mathbf{k}) - \Delta_A^2 (\langle \partial_{k_i} s_{\mathbf{k}} | \bar{s}_{\mathbf{k}} \rangle \langle \bar{s}_{\mathbf{k}} | \partial_{k_j} s_{\mathbf{k}} \rangle + (i \leftrightarrow j)) g(\mathbf{k}) \right]. \quad (33) \end{aligned}$$

where the functions  $f(\mathbf{k})$  and  $g(\mathbf{k})$  are defined as

$$f(\mathbf{k}) = (1 + \sin \phi_{\mathbf{k}})^2 \frac{\tanh(\beta E_{+,\mathbf{k}}/2)}{E_{+,\mathbf{k}}} + (1 - \sin \phi_{\mathbf{k}})^2 \frac{\tanh(\beta E_{-,\mathbf{k}}/2)}{E_{-,\mathbf{k}}} + 4 \frac{\tanh(\beta \Delta_A/2)}{\Delta_A} + 4 \cos^2 \phi_{\mathbf{k}} \frac{t_{-,\mathbf{k}}}{E_{+,\mathbf{k}} - E_{-,\mathbf{k}}}, \quad (34)$$

$$g(\mathbf{k}) = 2(1 - \sin \phi_{\mathbf{k}}) \frac{\tanh(\beta E_{-,\mathbf{k}}/2) - \tanh(\beta \Delta_A/2)}{E_{-,\mathbf{k}} - \Delta_A} + 2(1 + \sin \phi_{\mathbf{k}}) \frac{\tanh(\beta E_{+,\mathbf{k}}/2) + \tanh(\beta \Delta_A/2)}{E_{+,\mathbf{k}} + \Delta_A}. \quad (35)$$

One can distinguish the two gauge-invariant superfluid weight contributions. The conventional contribution  $D_{s,\text{conv}}$  is the one given by the first two terms in square brackets in Eq. (33) (first line). At half-filling this contribution is highly suppressed due to the vanishing density of states of the dispersive bands as it can be seen in Figs. 4(c)-(d) in the main text. The terms where the spinors  $|s_{\mathbf{k}}\rangle, |\bar{s}_{\mathbf{k}}\rangle$  and their derivatives appear represent the geometric contribution  $D_{s,\text{geom}}$ .

The main advantage of Eqs. (33)-(35) is that it is possible to single out the flat-band contribution  $D_{s,\text{geom}}|_{\text{f.b.}} = D_s|_{\text{f.b.}}$  to the superfluid weight (highlighted in red) from the geometric contribution associated to the other bands  $D_{s,\text{geom}}|_{\text{o.b.}}$ . Formally, one considers the isolated flat-band limit  $0 < \frac{U}{J} \ll \delta < 1$  which means that pairing occurs in the flat band only. In this limit one can set  $\sin \phi_{\mathbf{k}} = t_{-, \mathbf{k}} = 0$  and all terms of order  $\Delta_A/E_{\pm, \mathbf{k}} \approx U/(J\delta)$  are discarded. Then one obtains

$$\begin{aligned} [D_s]_{i,j} &= [D_{s,\text{geom}}|_{\text{f.b.}}]_{i,j} = \frac{\Delta_A}{\pi \hbar^2} \tanh \frac{\beta \Delta_A}{2} \frac{1}{2\pi} \int_{\text{B.Z.}} d^2 \mathbf{k} \text{Re}(\mathcal{B}_{ij}(\mathbf{k})|_{\text{f.b.}}) \\ &= \frac{\Delta_A}{\pi \hbar^2} \tanh \frac{\beta \Delta_A}{2} \mathcal{M}_{ij}^{\text{R}}|_{\text{f.b.}} = \frac{2}{\pi \hbar^2} \frac{\Delta_A^2}{U n_\phi} \mathcal{M}_{ij}^{\text{R}}|_{\text{f.b.}}. \end{aligned} \quad (36)$$

If the term corresponding to the upper and lower bands is neglected, the gap equation (26) reduces to  $\Delta_A = \frac{U n_\phi}{2} \tanh \frac{\beta \Delta_A}{2}$ . This result has been used in the last equality of Eq. (36). Eq. (36) is consistent with the general result for the superfluid weight at finite temperature in the flat-band limit as provided in Ref. [1]. This is rather surprising since one assumption has been made in the derivation of this result in Ref. [1], namely that the order parameters are all equal  $\Delta_\alpha = \Delta$ , but this condition is not satisfied in the case of the Lieb lattice where  $\Delta_A = \Delta_C \neq \Delta_B$ . This can be traced back to the fact that when the derivatives of Eq. (24) are taken all the terms proportional to  $\Delta_B$  drop out, a peculiar feature of the Lieb lattice. Eq. (36) can be extended away from half-filling by using the block structure of the Bogoliubov de-Gennes Hamiltonian (5) (see also Eq. (21)). The  $2 \times 2$  block corresponding to the flat band is diagonalized and the corresponding quasiparticle energies  $E_{0,\mathbf{k}} = E_0 = \sqrt{\mu^2 + \Delta_A^2}$  and coherence factors  $u_0 = 2^{-1/2} \sqrt{1 - \mu/E_0}$ ,  $v_0 = 2^{-1/2} \sqrt{1 + \mu/E_0}$  are obtained. Then inserting this result in Eqs. (16)-(17)-(18) and retaining the terms where only  $E_0, u_0, v_0$  appear (the ones highlighted in red in Eqs. (33)-(35)) leads to the result shown in Eqs. (3) in the main text.

The staggered hopping parametrized by  $\delta$  breaks the symmetry of the square lattice with respect to rotations by  $90^\circ$ . This means that  $\mathcal{M}_{ij}^{\text{R}}|_{\text{f.b.}}$  is not a diagonal matrix for  $\delta \neq 0$ , but has a nonzero off-diagonal component  $\mathcal{M}_{xy}^{\text{R}}|_{\text{f.b.}}$  while the diagonal components are equal  $\mathcal{M}_{xx}^{\text{R}}|_{\text{f.b.}} = \mathcal{M}_{yy}^{\text{R}}|_{\text{f.b.}}$ . The components of  $\mathcal{M}_{ij}^{\text{R}}|_{\text{f.b.}}$  are shown in Fig. 5 of the main text as a function of  $\delta$ . The off-diagonal elements are finite for all  $\delta$ , while the diagonal ones have a logarithmic singularity for  $\delta = 0$ . This singularity is due to the fact that the periodic Bloch functions are nonanalytic functions of the wavevector at the band intersection  $\mathbf{k}a = (\pi, \pi)^T$  for  $\delta = 0$ . This signals that other bands have to be included in order to compute the superfluid weight.

The various contributions to the superfluid weight are shown in Fig. 4(a)-(d) in the main text. On the other hand, in Fig. 6 we compare the total superfluid weight for different values of the staggering parameter  $\delta$  at zero temperature. We find that for large  $\delta$  the superfluid weight is linear in  $U$ , a fact that is explained by the dominant role of the flat band when the energy gap  $E_g$  is much larger than  $U$ . Indeed Eq. (36) gives the slope of  $D_s$  around  $U = 0$ . On the contrary, for small  $\delta$  pronounced deviations from linearity can be seen, an effect due to the other bands geometric contribution  $D_{s,\text{geom}}|_{\text{o.b.}}$ . At  $\delta = 0$  this implies that the superfluid weight has a diverging derivative at  $U = 0$ . However, the negative contribution from the other bands ensures that the superfluid weight is finite even at  $\delta = 0$ .

Note how the diagonal components  $[D_s]_{x,x} = [D_s]_{y,y}$  are decreasing functions of  $\delta$ , while for  $\delta = 0$  the off-diagonal elements are zero due to rotational symmetry, and their magnitude increases with  $\delta$ . Eventually, for  $\delta = 1$  the superfluid weight tensor has a zero eigenvalue which implies that the superconducting state is unstable (see Fig. 5 in the main text). Indeed, long-range order cannot be established since the unit cells as defined in Fig. 1 in the main text are decoupled. However, the value of the order parameter  $\Delta_A$  is essentially unaffected at the mean-field level when changing  $\delta$  as shown in Fig. 3 in the main text. This unphysical behavior is due to the fact that MF captures thermally excited quasiparticles, but not the thermal fluctuations of the order parameter phase or other collective modes. The collective mode fluctuations are the ones responsible for the collapse of the superconductive order with increasing  $\delta$  and they are captured by Dynamical Mean Field Theory to some extent (see below).

## Appendix B: Exactness of the BCS wavefunction in the isolated flat-band limit

In this section we prove that in case of an isolated flat band ( $U \ll E_{\text{gap}}$ ) the BCS wavefunction describing superconductivity becomes an exact ground state for a large class of interaction terms. We start by considering a Hamiltonian

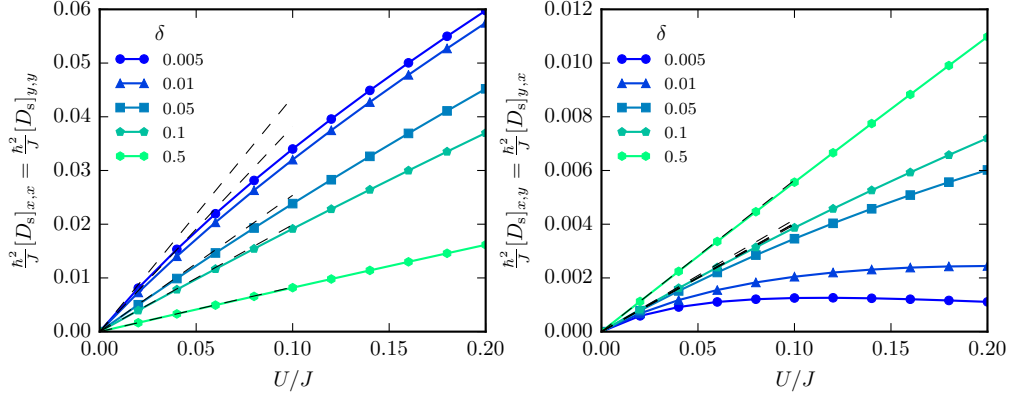


FIG. 6. Total superfluid weight as function of  $U/J$  for different values of the staggering parameter  $\delta$  at zero temperature  $T = 0$ . The diagonal components of the superfluid weight tensor are shown in the left panel while the off-diagonal ones are shown in the right panels. For large  $\delta$  the superfluid weight is linear in  $U$  since the flat band contribution is dominating. The black dashed line represents the flat band contribution Eq. (36). Deviations from linearity are more pronounced for small  $\delta$  since the geometric contribution of the other bands plays an increasingly important role.

with *repulsive* interaction

$$\hat{\mathcal{H}} = \hat{\mathcal{H}}_{\text{kin}} + \hat{\mathcal{H}}_{\text{int}} = \hat{\mathcal{H}}_{\text{kin}} + \sum_{\mathbf{i}\alpha, \mathbf{j}\beta} U(|\mathbf{r}_{\mathbf{i}\alpha} - \mathbf{r}_{\mathbf{j}\beta}|) \hat{n}_{\mathbf{i}\alpha} \hat{n}_{\mathbf{j}\beta}, \quad (37)$$

where  $\hat{\mathcal{H}}_{\text{kin}}$  is the kinetic term and the second term  $\hat{\mathcal{H}}_{\text{int}}$  describes the interaction between the particles. The interaction potential  $U(r)$  is assumed to be repulsive and  $\hat{n}_{\mathbf{i}\alpha} = \hat{n}_{\mathbf{i}\alpha\uparrow} + \hat{n}_{\mathbf{i}\alpha\downarrow}$  is the particle number operator of the lattice site located at position  $\mathbf{r}_{\mathbf{i}\alpha}$ . The interaction term is invariant under rotations in spin space and we require that the same holds for  $\hat{\mathcal{H}}_{\text{kin}}$ . We also assume that the noninteracting Hamiltonian  $\hat{\mathcal{H}}_{\text{kin}}$  contains a band which is strictly flat and isolated from other bands by a finite band gap  $E_{\text{gap}}$ . This band is labelled by  $\bar{n}$ . If the flat band is partially filled and the interaction is small compared to the band gap it is a good approximation to retain only the flat band states in the expansion of the annihilation operators

$$\hat{c}_{\mathbf{i}\alpha\sigma} = \sum_n \sum_{\mathbf{k}} e^{i\mathbf{k}\cdot\mathbf{r}_{\mathbf{i}\alpha}} g_{n\mathbf{k}}(\alpha) \hat{c}_{n\mathbf{k}\sigma} \approx \sum_{\mathbf{k}} e^{i\mathbf{k}\cdot\mathbf{r}_{\mathbf{i}\alpha}} g_{\bar{n}\mathbf{k}}(\alpha) \hat{c}_{\bar{n}\mathbf{k}\sigma}, \quad (38)$$

and the same can be done for the creation operators  $\hat{c}_{\mathbf{i}\alpha\sigma}^\dagger$ . The Bloch function  $g_{\bar{n}\mathbf{k}}$  are independent of spin owing to the spin rotational symmetry of  $\hat{\mathcal{H}}_{\text{kin}}$ . Inserting this last equation in Eq. (37) and after some manipulations, the Hamiltonian takes the form

$$\hat{\mathcal{H}} = \hat{\mathcal{H}}_{\text{int}} + \text{const.} = \frac{1}{(2\pi)^2} \int d^2\mathbf{q} u(\mathbf{q}) (\hat{\rho}_\uparrow^\dagger(\mathbf{q}) + \hat{\rho}_\downarrow^\dagger(\mathbf{q})) (\hat{\rho}_\uparrow(\mathbf{q}) + \hat{\rho}_\downarrow(\mathbf{q})) + \text{const.} \quad (39)$$

where the Fourier transform  $\hat{\rho}_\sigma(\mathbf{q})$  of the density operator projected in the flat-band subspace is given by

$$\hat{\rho}_\sigma(\mathbf{q}) = \hat{\rho}_\sigma^\dagger(-\mathbf{q}) = \sum_{\mathbf{k}} c_{\bar{n}\mathbf{k}\sigma}^\dagger c_{\bar{n}(\mathbf{k}+\mathbf{q})\sigma} \sum_{\alpha} g_{\bar{n}\mathbf{k}}^*(\alpha) g_{\bar{n}(\mathbf{k}+\mathbf{q})}(\alpha) = \sum_{\mathbf{k}} c_{\bar{n}\mathbf{k}\sigma}^\dagger c_{\bar{n}(\mathbf{k}+\mathbf{q})\sigma} \langle g_{\bar{n}\mathbf{k}} | g_{\bar{n}(\mathbf{k}+\mathbf{q})} \rangle, \quad (40)$$

and  $u(\mathbf{q})$  is the Fourier transform of the potential  $U(|\mathbf{r}|) = (2\pi)^{-2} \int d^2\mathbf{q} u(\mathbf{q}) e^{i\mathbf{q}\cdot\mathbf{r}}$ . For a flat band the noninteracting term is a trivial constant that can be dropped from Eq. (39). Since  $\rho_\sigma(\mathbf{q} = 0) = \hat{N}_\sigma$  is the operator counting the number of particles with spin  $\sigma$ , the  $\mathbf{q} = 0$  term in Eq. (39) can be dropped as well without affecting the physical properties of the system. The Hamiltonian (39) is a positive definite operator provided that the Fourier transform of the interaction potential  $u(\mathbf{q})$  is a positive number, which is the case for a repulsive potential. It is easy to show that the completely polarized ferromagnetic state, which has the form  $|\text{Ferro}\rangle = \prod_{\mathbf{k}} (u \hat{c}_{\bar{n}\mathbf{k}\downarrow}^\dagger + v \hat{c}_{\bar{n}\mathbf{k}\uparrow}^\dagger) |0\rangle$ , is annihilated by the total projected density operator  $\hat{\rho}(\mathbf{q}) = \hat{\rho}_\uparrow(\mathbf{q}) + \hat{\rho}_\downarrow(\mathbf{q})$  for  $\mathbf{q} \neq 0$ , namely  $\hat{\rho}(\mathbf{q})|\text{Ferro}\rangle = 0$ . Therefore the ferromagnetic state is a zero energy eigenstate of the Hamiltonian ( $\hat{\mathcal{H}}|\text{Ferro}\rangle = 0$ ) if all terms proportional to the

particle number operators  $\hat{N}_\sigma$  are dropped. Since  $\hat{\mathcal{H}}$  can have only nonnegative eigenvalues, the ferromagnetic state is a ground state with a trivial degeneracy given by the spin symmetry. Indeed the only restriction on the complex coefficients  $u, v$  is  $|u|^2 + |v|^2 = 1$ . Now the particle-hole transformation of the down spin given in the main text,  $\hat{c}_{\bar{n}\mathbf{k}\downarrow} \rightarrow \hat{c}_{\bar{n}(-\mathbf{k})\downarrow}^\dagger$ , is applied to the ferromagnetic wavefunction. The vacuum state transforms as  $|0\rangle \rightarrow \prod_{\mathbf{k}} \hat{c}_{\bar{n}(-\mathbf{k})\downarrow}^\dagger |0\rangle$ , while the ferromagnetic state becomes the BCS wavefunction

$$\begin{aligned} |\text{Ferro}\rangle &\rightarrow \prod_{\mathbf{k}} \left( u \hat{c}_{\bar{n}(-\mathbf{k})\downarrow} + v \hat{c}_{\bar{n}\mathbf{k}\uparrow}^\dagger \right) \prod_{\mathbf{k}'} c_{\bar{n}(-\mathbf{k}')\downarrow}^\dagger |0\rangle = \prod_{\mathbf{k}} \left[ \left( u \hat{c}_{\bar{n}(-\mathbf{k})\downarrow} + v \hat{c}_{\bar{n}\mathbf{k}\uparrow}^\dagger \right) \hat{c}_{\bar{n}(-\mathbf{k})\downarrow}^\dagger \right] |0\rangle \\ &= \prod_{\mathbf{k}} \left( u + v \hat{c}_{\bar{n}\mathbf{k}\uparrow}^\dagger \hat{c}_{\bar{n}(-\mathbf{k})\downarrow}^\dagger \right) |0\rangle = |\text{BCS}\rangle. \end{aligned} \quad (41)$$

Note that if we use the parametrization  $u = \sqrt{1-\nu}$  and  $v = e^{i\phi}\sqrt{\nu}$ , then  $\nu$  is the flat-band filling and  $e^{i\phi}$  is the arbitrary phase of the superconducting order parameter. Furthermore, under the particle-hole transformation, the Hamiltonian projected on the flat band subspace (39) becomes

$$\hat{\mathcal{H}} \rightarrow \hat{\mathcal{H}}' = \frac{1}{(2\pi)^2} \int d^2\mathbf{q} u(\mathbf{q}) (\hat{\rho}_\uparrow^\dagger(\mathbf{q}) - \hat{\rho}_\downarrow^\dagger(\mathbf{q})) (\hat{\rho}_\uparrow(\mathbf{q}) - \hat{\rho}_\downarrow(\mathbf{q})) + \text{const.}, \quad (42)$$

where the density operators  $\hat{\rho}_\sigma(\mathbf{q})$  are

$$\hat{\rho}_\sigma(\mathbf{q}) = \hat{\rho}_\sigma^\dagger(-\mathbf{q}) = \sum_{\mathbf{k}} c_{\bar{n}\mathbf{k}\sigma}^\dagger c_{\bar{n}(\mathbf{k}+\mathbf{q})\sigma} \langle g_{\bar{n}\mathbf{k}\sigma} | g_{\bar{n}(\mathbf{k}+\mathbf{q})\sigma} \rangle. \quad (43)$$

The only difference with Eq. (40) is that the Bloch functions are spin-dependent. Indeed the spin rotational symmetry of  $\hat{\mathcal{H}}_{\text{kin}}$  implies that after the particle-hole transformation the Bloch functions are time-reversal symmetric  $g_{\bar{n}\mathbf{k}\uparrow} = g_{\bar{n}(-\mathbf{k})\downarrow}^*$ , but in general spin rotational symmetry is lost. It can be easily verified that the BCS state is a zero eigenstate of the Hamiltonian  $\hat{\mathcal{H}}'$  since  $(\hat{\rho}_\uparrow(\mathbf{q}) - \hat{\rho}_\downarrow(\mathbf{q}))|\text{BCS}\rangle = 0$  for  $\mathbf{q} \neq 0$ . This last identity is obtained from  $\hat{\rho}(\mathbf{q})|\text{Ferro}\rangle = 0$  using the particle-hole transformation. It is also an instructive exercise to verify it directly from (43) using the time-reversal symmetry of the Bloch functions. Therefore the BCS wavefunction is a zero eigenstate of  $\hat{\mathcal{H}}'$ , i.e. a ground state (again all terms proportional to  $\hat{N}_\sigma$  are neglected). The Hamiltonian  $\hat{\mathcal{H}}'$  is obtained by projection on the flat-band subspace of the interaction term  $\sum_{\mathbf{i}\alpha, \mathbf{j}\beta} U(|\mathbf{r}_{\mathbf{i}\alpha} - \mathbf{r}_{\mathbf{j}\beta}|) (\hat{n}_{\mathbf{i}\alpha\uparrow} - \hat{n}_{\mathbf{i}\alpha\downarrow})(\hat{n}_{\mathbf{j}\beta\uparrow} - \hat{n}_{\mathbf{j}\beta\downarrow})$ , which is repulsive for particle with same spins and attractive for opposite spins. In the case of a contact potential  $U(|\mathbf{r}_{\mathbf{i}\alpha} - \mathbf{r}_{\mathbf{j}\beta}|) = U\delta_{\mathbf{i}\alpha, \mathbf{j}\beta}$  this interaction is equivalent to an attractive Hubbard interaction, due to the Pauli exclusion principle. It is important to note that the particle-hole transformation can be used only in case of a perfectly flat dispersion otherwise it has a nontrivial effect on the kinetic term. Moreover this transformation is different from the one introduced by Emery which is a mapping between attractive and repulsive Hubbard models in a bipartite lattice [4]. Indeed our argument it can be applied to lattices with flat bands that are not bipartite, such as the kagome lattice.

The result provided here tells that the BCS state is one of the ground states for an attractive Hubbard interaction, but this alone does not guarantee superconductivity. A simple counterexample is provided by our model on the Lieb lattice with  $\delta = 1$ , which is obviously not superconducting. The criteria for superconductivity is a finite superfluid weight which is related to the quantum metric, an invariant of the flat band. More precisely the superfluid weight tensor must be non-singular. However a finite superfluid weight guarantees only the local stability of the BCS ground state and one cannot rule out the existence of other competing ground states. Using Lieb theorem [6] and the particle-hole transformation introduced here, it is possible to show that the BCS ground state is unique in the case of the model considered in this work, when the flat band is well isolated from other bands and partially filled. Indeed, for the Lieb lattice with repulsive Hubbard interaction at half-filling, Lieb theorem states that the total spin  $S$  of the ground state is given by  $2S = N_A + N_C - N_B$  where  $N_\alpha$  is the number of lattice sites in the  $\alpha$  sublattice. The lower filled band can be neglected in the limit  $U \ll E_g$  and, since the  $2S$  electrons in the half-filled flat band have total spin  $S$ , the ground state can only be the ferromagnetic state  $|\text{Ferro}\rangle$ . The uniqueness of the BCS ground state at any filling of the flat band follows again by particle-hole transformation. The numerical results presented in the main text and in the following show that the BCS wavefunction is in fact a good approximation even when the flat band is not isolated.

### Appendix C: Comparison between mean field BCS theory and dynamical mean field theory

To check the validity of our MF theory, we apply cellular dynamical mean-field theory [7–9] with the continuous-time interaction expansion (CT-INT) impurity solver [10, 11]. In our computations the impurity problem is chosen to



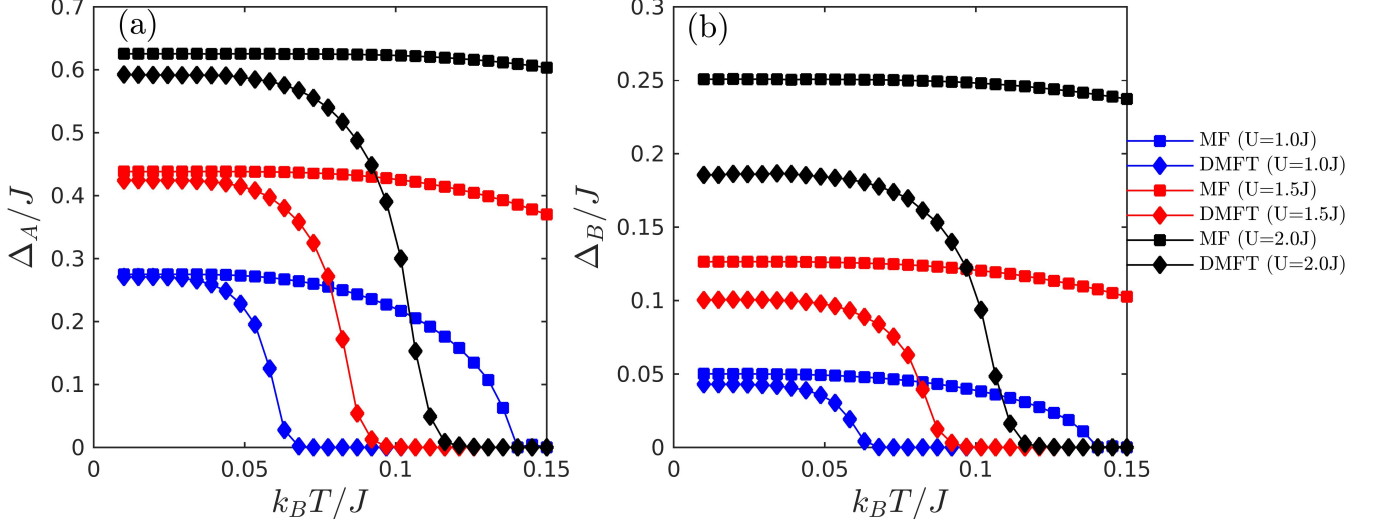


FIG. 7. Order parameters  $\Delta_A$  (a) and  $\Delta_B$  (b) for half-filled flat band computed by using DMFT and MF as a function of temperature  $T$ . The results are provided for three different interaction strengths. The data is for hopping coefficients without staggering ( $\delta = 0$ ).

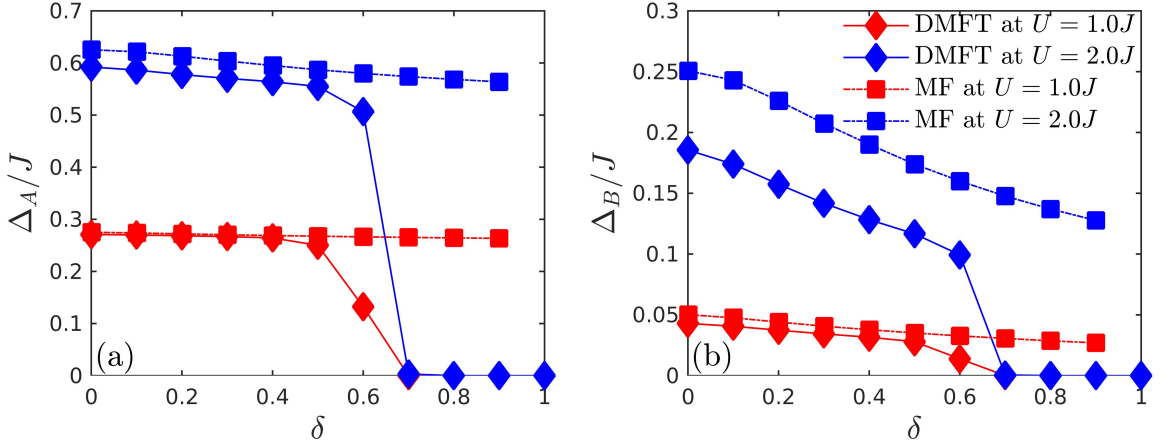


FIG. 8. Order parameters  $\Delta_A$  (a) and  $\Delta_B$  (b) of half-filled flat band as a function of  $\delta$  obtained by using MF (squares) and DMFT (diamonds) for two different interaction strengths ( $U = 1.0J$  and  $U = 2.0J$ ). Here the temperature is set to  $k_B T = 0.01J$ .

consists of the three lattice sites within one unit cell which is then coupled self-consistently to the rest of the lattice. Inside the unit cell the correlations are treated exactly, whereas the coupling to the environment is treated at the mean-field level.

In Fig. 7 we compare MF with DMFT for half-filled flat band and three different interaction strengths  $U = 1.0J, 1.5J, 2.0J$  by presenting the order parameters  $\Delta_A$  and  $\Delta_B$  as a function of the temperature. We see that at high temperatures MF deviates notably from DMFT and overestimates the critical temperatures. Indeed, MF neglects thermal fluctuations of the order parameter phase as discussed in Section , while they are included to a certain extent in DMFT. On the other hand, at lower temperatures the agreement between the two methods is good, especially in case of  $\Delta_A$ . Because superfluidity in the flat band is related to a finite  $\Delta_A$  rather than  $\Delta_B$ , we deduce that at low temperatures the MF approach is reliable when investigating the superconductive properties of the flat band.

We further compare the two methods in Fig. 8 where we plot  $\Delta_A$  and  $\Delta_B$  as a function of the staggering parameter  $\delta$  obtained by MF and DMFT for two different interaction values,  $U = 1.0J$  and  $U = 2.0J$ . This is the same plot as

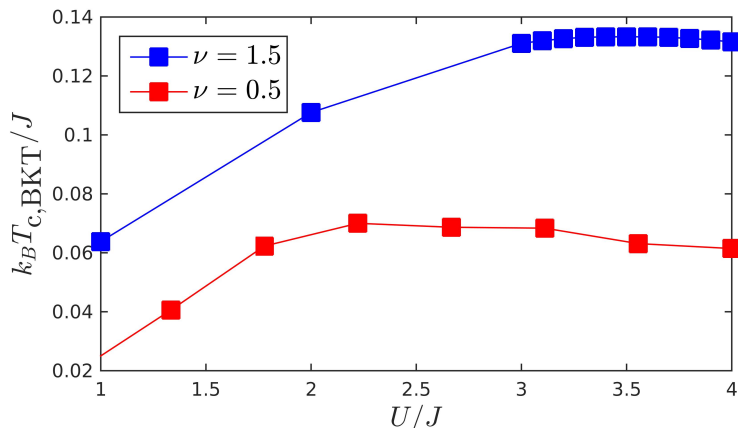


FIG. 9. BKT transition temperatures for half-filled flat band ( $\nu = 1.5$ ) and half-filled lower dispersive band ( $\nu = 0.5$ ) as a function  $U$ . The staggering parameter is fixed to  $10^{-3}$ .

in Fig. 2 in the main text where  $U = 0.4J$ . One can see that, especially in case of  $\Delta_A$ , MF is in good agreement with DMFT even for larger  $U$ . Compared to the results in Fig. 2 of the main text, we also see that now the order parameter values computed by using DMFT are finite for larger staggering values. This is expected since the superfluid weight increases approximately linearly with the interaction strength and the system becomes correspondingly more robust against thermal fluctuations of the order parameter phase.

#### Appendix D: Berezinsky-Kosterlitz-Thouless transition temperatures

In two dimensions the Berezinsky-Kosterlitz-Thouless (BKT) transition temperature  $T_{c,\text{BKT}}$  is defined by a well-known universal relation [12] that in our units reads

$$\frac{\hbar^2}{4} D_s(T_{c,\text{BKT}}) = \frac{2}{\pi} k_B T_{c,\text{BKT}}. \quad (44)$$

We use this formula to compute the transition temperature in our system, where the superfluid weight as a function of temperature  $D_s(T)$  is obtained from MF. In Fig. 9 we present  $T_{c,\text{BKT}}$  as a function of  $U$  for half filled flat band ( $\nu = 1.5$ , blue curve) and for approximately half-filled lower dispersive band ( $\nu \approx 0.5$ , red curve) which is equivalent to half-filled upper dispersive band due to particle-hole symmetry of bipartite lattices. To compute the case  $\nu = 0.5$  one has to adjust the chemical potential  $\mu$  for each value of  $U$  in order to obtain the required filling for the dispersive band. This causes the small unphysical oscillations seen in the plot. One sees from Fig. 9 that the flat band yields higher transition temperatures by at least a factor of two in comparison with the dispersive bands. The transition temperature is maximized for the flat band around  $U \approx 3.5J$  which yields the value  $T_{c,\text{BKT}} \approx 0.133J$ , whereas for the dispersive band the maximum occurs at  $U \approx 2.2J$  with the value  $T_{c,\text{BKT}} \approx 0.07J$ . The maximum in the BKT critical temperature coincides approximately with the maximum in the superfluid weight (see Fig. 4(a) in the main text).

---

\* paivi.torma@aalto.fi

- [1] S. Peotta and P. Törmä, *Nature Communications* **6**, 8944 (2015).
- [2] Grosso, G. & Parravicini, G. P., *Solid State Physics*, 2nd ed., Elsevier (2014).
- [3] V. I. Iglovikov, F. Hébert, B. Grémaud, G. G. Batrouni, and R. T. Scalettar *Phys. Rev. B* **90**, 094506 (2014).
- [4] V. J. Emery, *Phys. Rev. B* **14**, 2989 (1976).
- [5] E. H. Lieb, M. Loss, R. J. McCann, *Journal of Mathematical Physics* **34**, 891 (1993).
- [6] E. H. Lieb, *Phys. Rev. Lett.* **62**, 1201 (1989).
- [7] A. Georges and G. Kotliar and W. Krauth and M. J. Rozenberg, *Rev. Mod. Phys.* **68**, 13-125 (1996).
- [8] T. Maier and M. Jarrell and T. Pruschke and M. H. Hettler, *Rev. Mod. Phys.* **77**, 1027-1080 (2005).
- [9] G. Kotliar and S. Y. Savrasov and G. Pálsson and G. Biroli, *Phys. Rev. Lett.* **87**, 186401 (2001)

- [10] A. N. Rubtsov, V. V. Savkin, and A. I. Lichtenstein, [Phys. Rev. B](#) **72**, 035122 (2005).
- [11] E. Gull, A. J. Millis, A. I. Lichtenstein, A. N. Rubtsov, M. Troyer, and P. Werner, [Rev. Mod. Phys.](#) **83**, 349 (2011).
- [12] D. R. Nelson and J. M. Kosterlitz, [Phys. Rev. Lett.](#) **39**, 1201-1204 (1977).